RF Project 715430/763646
Final Report

(NASA-CR-176104) DIFFUSION WELDING OF CASSEGRAINIAN CONCENTRATOR CELL STACK ASSEMBLIES M.S. Thesis Final Report, Jun. 1983 - Sep. 1985 (Ohio State Univ., Columbus.) 137 p HC A07/MF A01 CSCL 10B G3/44

N85-33566

Unclas
22123

# FEASIBILITY STUDY ON DIFFUSION BONDING IN GaAs SOLAR CELL FABRICATION

Charles E. Albright
Department of Welding Engineering

# DIFFUSION WELDING OF CASSEGRAINIAN CONCENTRATOR CELL STACK ASSEMBLIES

by
Kenneth John Gangl

For the Period
June 1983 - September 1985

NATIONAL AERONAUTICS AND SPACE ADMINISTRATION
Lewis Research Center
21000 Brookpark Road
Cleveland, Ohio 44135

Grant No. NAG3-448

July 1985


OSU
The Ohio State University
Research Foundation
1314 Kinnear Road
Columbus, Ohio 43212

# DIFFUSION WELDING OF CASSEGRAINIAN CONCENTRATOR CELL STACK ASSEMBLIES

# DIFFUSION WELDING OF
# CASSEGRAINIAN CONCENTRATOR
# CELL STACK ASSEMBLIES

A Thesis

Presented in Partial Fulfillment of the Requirements
for the Degree Master of Science, Welding Engineering

by

Kenneth John Gangl, B.S.W.E.

The Ohio State University
1985

Approved by

---

Advisor

Department of Welding Engineering

THESIS ABSTRACT

THE OHIO STATE UNIVERSITY
GRADUATE SCHOOL

NAME: Kenneth J. Gangl QUARTER/YEAR: Spring 1985

DEPARTMENT: Welding Eng. DEGREE: Master of Science

TITLE OF THESIS: Diffusion Welding of Cassegrainian Concentrator Cell Stack Assemblies.


The purpose of the present study was to begin development of a procedure to join the components of the Cassegrainian concentrator photovoltaic cell stack assembly. Diffusion welding was selected as the most promising process, and was concentrated on exclusively.

All faying surfaces were coated with silver to promote welding. The first phase of the study consisted of developing the relationship between process parameters and joint strength using silver plated steel samples and an isostatic pressure system. In the second phase, mockups of the cell stack assembly were welded in a hot isostatic press. Excellent joint strength was achieved with parameters of 350 °C and 10 ksi, but the delicate GaAs component could not survive the welding cycle without cracking. The tendency towards cracking was found to be affected by both temperature and pressure. Further work will be required in the future to solve this problem.


Advisor's Signature

## TABLE OF CONTENTS

## List of Figures

## LIST OF TABLES

## INTRODUCTION

Historically, the emphasis in designing space based photovoltaic systems seems to have been on improving cell efficiency and lowering overall weight. With the large power requirements projected for the space station, however, the National Aeronautics and Space Administration (NASA) is now considering systems which will lower costs as well as improve efficiency. TRW's Space Group has been commissioned by NASA to design a system which uses inexpensive optics to concentrate incident sunlight, allowing a corresponding decrease in the semiconductor area required for a given power output.[1] Since the semiconductor material is by far the most expensive component of a solar array, the concentrator system has the potential to significantly reduce the overall system cost. The present study is concerned with developing a joining procedure for the concentrator system which will meet the design requirements without detracting from the cost advantage.

The TRW design, shown in figure 1, is simply a Cassegrainian reflector system.[1] The incident solar light strikes a parabolic mirror and is focused and reflected up to a smaller hyperbolic mirror. The smaller mirror then directs the light down through a "light

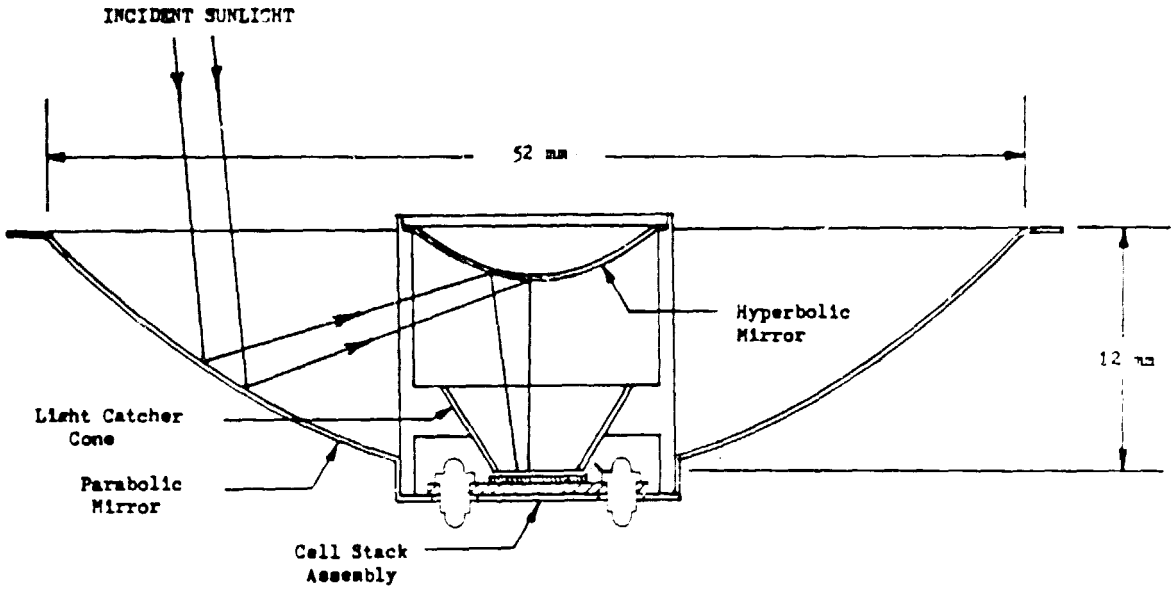


**Figure 1: Cross sectional view of Cassegrainian reflector system.**

catcher cone" to the photovoltaic cell. The incident sunlight is thus concentrated by about 100 times.[1]

The photovoltaic cell stack assembly, shown enlarged in figure 2, is the portion of the system requiring a joining procedure. At the top of the stack is the photovoltaic cell, shown again in figure 3, which consists of a gallium arsenide (GaAs) substrate with several thin, vapor deposited metal layers. The metal layers together constitute the "ohmic contact," which is necessary for current flow between the semiconductor and the load circuit.[2] The combination of metals shown represents only the most likely of several possibilities for the ohmic contact. The contacts must be annealed to provide a controlled amount of interdiffusion, which makes them "ohmic."[3] The annealing temperature may vary from 350 to 600 C[5], and the holding time may run from a few seconds to several minutes.

The component at the bottom of the cell stack assembly in figure 2 is actually a portion of the parabolic mirror, but it also acts as a radiator of the heat generated in the cell. This component will be made of copper, coated with approximately 1200 angstroms of silver.

The component in the middle of the cell stack

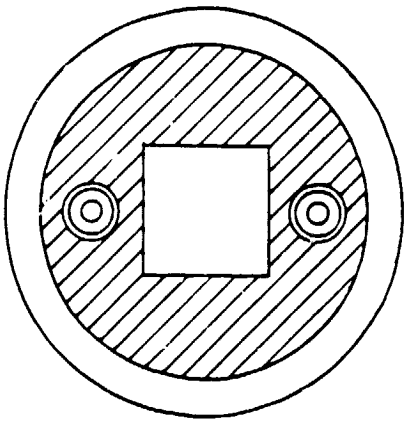

Top View

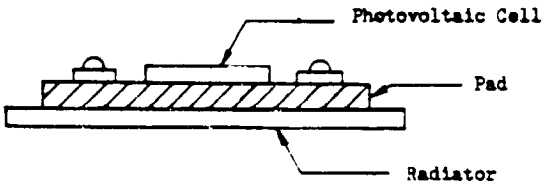


Cross Sectional View

**Figure 2: Enlarged view of photovoltaic cell stack assembly**

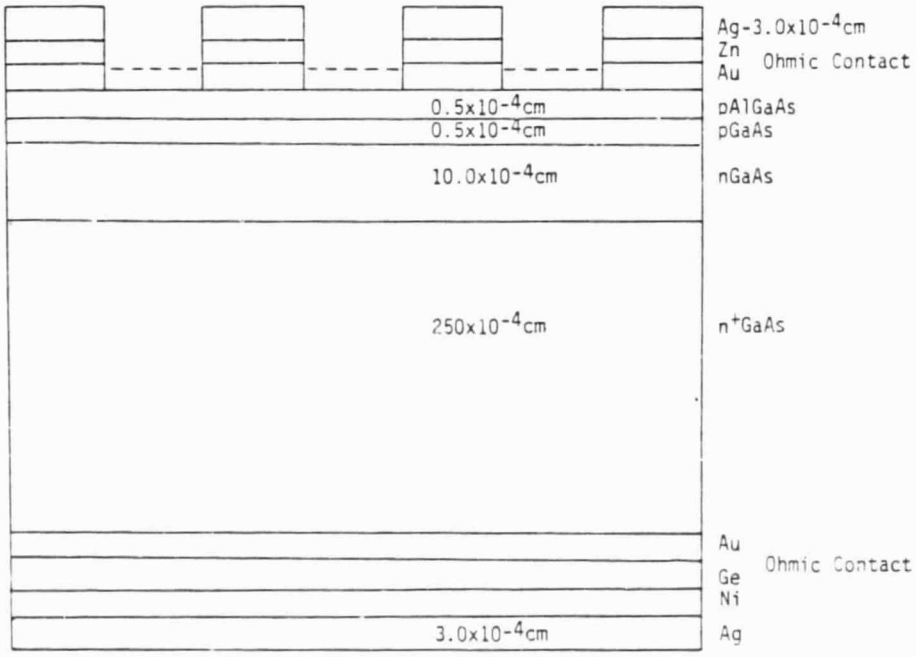


**Figure 3: Cross sectional view of GaAs Photovoltaic cell**

assembly, called the pad, will be made of a material with a low thermal expansion coefficient. The pad is intended to minimize the stress on the photovoltaic cell resulting from the thermal expansion mismatch between GaAs and Cu. Gallium arsenide has a thermal expansion coefficient of about $5 \times 10^{-6}$ $C^{-1}$ (6), whereas the coefficient for Cu is about $17 \times 10^{-6}$ $C^{-1}$ (6). When the parts are bonded together in the final assembly, temperature variations will produce stresses in each of the components. The pad is introduced to transfer some of the stress away from the photovoltaic cell, the most delicate and important element of the stack.

The effect of thermal stresses in service is made more severe by the fact that, once each orbit, the stack is subjected to a thermal cycle from -80 to +80 C. In a typical 10 year mission in low Earth orbit, the array will be required to withstand this temperature cycle about 60,000 times. Therefore, thermal fatigue is of primary concern.

The material of choice for the pad is presently beryllia (BeO), with a metallic material such as Kovar, Invar or molybdenum as a possible substitute. Beryllia is an attractive choice because it exhibits a unique combination of physical properties: low thermal

expansion, high thermal conductivity and high electrical resistivity.[7] The electrical insulation will allow the mirrors and support structure of the array to be isolated from the cells, which improves design flexibility.

In choosing a joining procedure for the Cassegrainian concentrator cell stack assembly, several criteria had to be considered:

1) The process must not require excessive heating or deformation of the parts.
2) The joints formed must exhibit good thermal fatigue resistance.
3) A large joint area must be provided for good thermal contact and strength.
4) The procedure must not be merely a laboratory exercise, but rather must be easily adaptable to production.

A review of the available joining methods with the above criteria in mind resulted in only two possibilities: soldering and diffusion welding. Relatively little experimental work has been performed in comparing the two processes, but the evidence which does exist indicates that diffusion welding has the potential to produce joints with superior fatigue

resistance.[8] For this reason, the present study has concentrated solely on diffusion welding.

The next chapter contains a review of the diffusion welding process, including the probable mechanisms involved. Also presented are the effects of welding conditions on the resulting bond strength, as determined by previous studies. The remainder of the report deals with the experimental work performed. The data base was first expanded by performing welds on steel coupons to simulate the actual joint assemblies. Further work was performed on assemblies approximating the TRW design. It was found that a significant sacrifice in strength was necessary to prevent cracking of the gallium arsenide layer. Recommendations were made which may resolve this problem with further study.

## BACKGROUND

### Diffusion Welding: Description and mechanisms

The American Welding Society (AWS) defines diffusion welding as "...a joining process wherein the principle mechanism for joint formation is solid state diffusion. Coalescence of the faying surfaces is accomplished through the application of pressure at elevated temperature. No melting and only limited macroscopic deformation or relative motion of the parts occurs during welding."[9] Though essentially correct, this definition requires further elaboration, particularly of the controlling mechanisms. In fact, four different processes have been identified which contribute in varying amounts to the formation of a diffusion weld: plastic deformation, recrystallization, creep and the diffusion of contaminants from the joint interface.[10,11,12] The latter three processes are indeed controlled by solid state diffusion. The relative importance of each mechanism is a function of the materials being joined and the welding parameters used.

All metals in the solid state exhibit a regular atomic order, or characteristic lattice structure,[13] as shown in figure 4. The spacing between lattice atoms is that distance which provides an equilibrium between

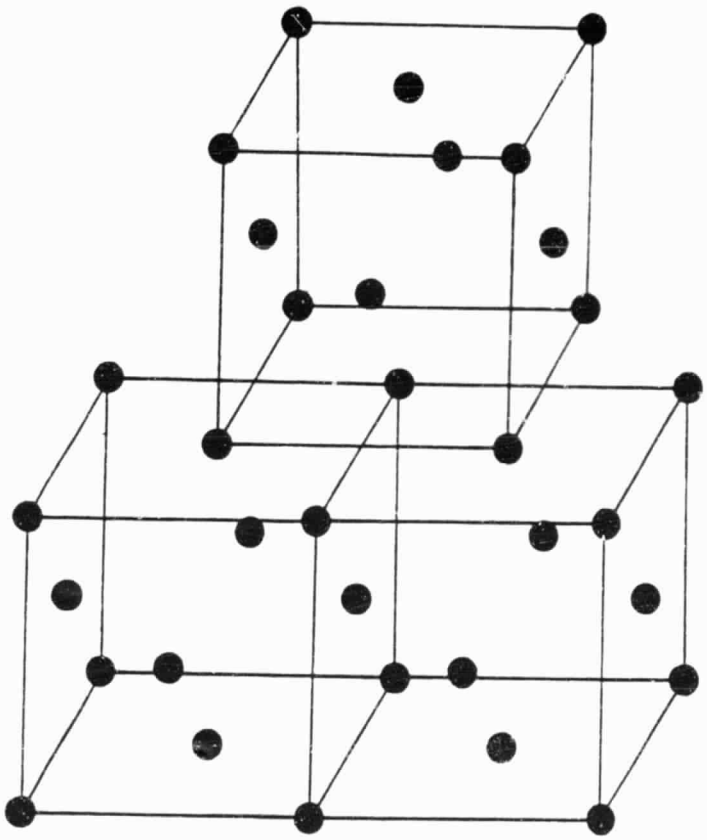

Figure 4: Schematic of typical metal lattice structure (face centered cubic).

attractive and repulsive interatomic forces.[14] Most metallic solids are composed of many small, discrete crystals called grains, which are distinguishable by their orientation. At the external surfaces of such a solid are atoms with less than a full complement of nearest neighbors.[10] The surface atoms will exert a cohesive force on those of another surface if the parts are brought within close proximity. Within 10 Angstroms (A) the cohesive force is very strong, but it decreases rapidly with further distance. Thus, the basic requirements for the formation of a weld between components are simply proximity of the opposing surfaces and atomic registry. The latter requirement is necessary because the strain on the lattice from a low angle boundary might weaken the weld.[15]

Plastic Deformation. Because the external force applied during diffusion welding is concentrated in the small regions of contact, the stress is relatively high and the surface asperities are plastically deformed.[16,17] The deformation which occurs is on a microscopic level, and thus does not constitute "relative motion" of the parts. As the asperities are crushed, the area of contact increases and clean metal is extruded through the contamination layer. The

deformation is promoted by the elevated temperature used in diffusion welding, as yield strength usually decreases with increased temperature. Eventually, the contact area increases to a level where the stress is no longer sufficient to cause plastic deformation. This generally occurs before 100% contact is achieved. The joint then looks somewhat as shown in figure 5, with scattered areas of good bonding, but numerous voids and contamination remaining. These remaining defects must be removed by diffusion dominated mechanisms.

Creep. Creep may be defined as the progressive deformation of a metal when subjected to a constant stress over a period of time.(18) Some of the strain is recoverable with time after the stress is released, but a significant portion is not recoverable. Metals have generally been found to exhibit significant creep at temperatures above 0.3 Tm (where Tm is the absolute melting temperature). Creep has often been proposed as a major factor in the elimination of voids remaining after plastic deformation has ceased.(19,20,)

Creep is generally considered to occur in three stages, as shown graphically in figure 6.(21) Primary creep is a period of decreasing creep rate during which an increase in dislocation density due to deformation is

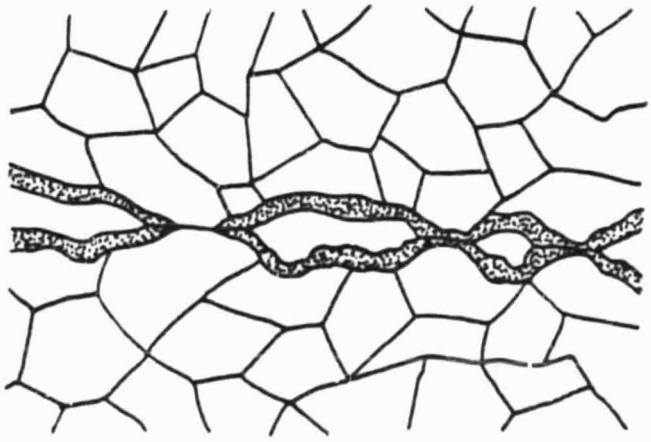

Figure 5: Cross sectional representation of diffusion welded joint after microscopic plastic deformation has ceased.

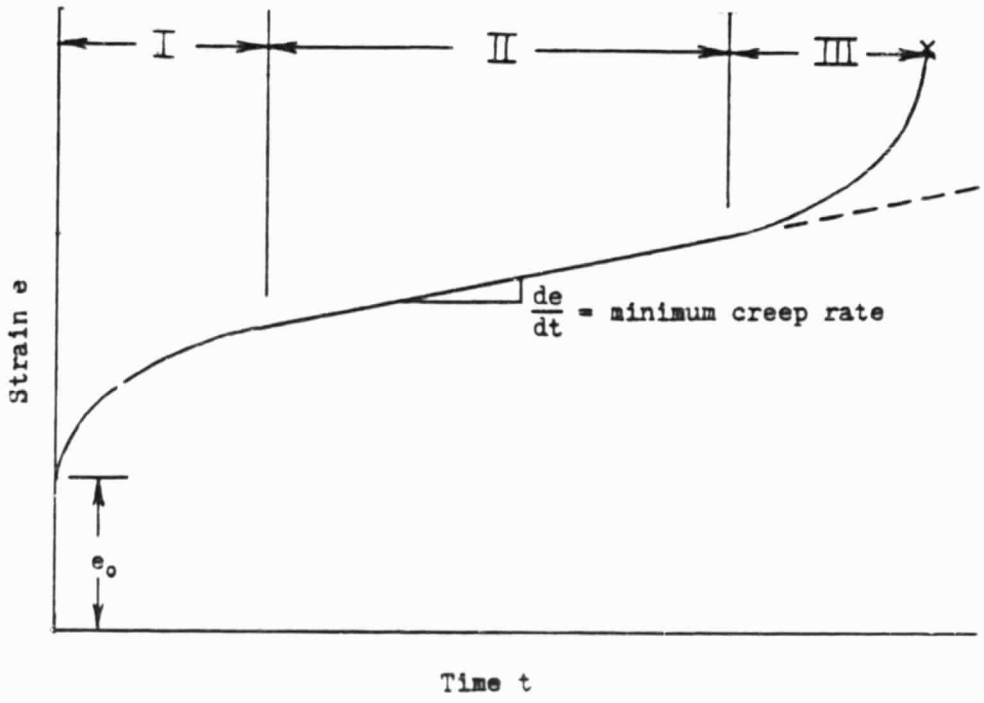


Figure 6: Three stages of creep

responsible for increasing the resistance to creep. Secondary, or steady-state creep, represents a period of nearly constant creep rate during which strain hardening and recovery balance out. Tertiary creep consists of an accelerated creep rate which leads to failure in tensile creep samples.

The stage of creep which will predominate in diffusion welding is primarily determined by the homologous temperature, $T/T_m$ (where T is the welding temperature). At very low homologous temperatures, recovery is impossible and primary creep dominates. At somewhat higher temperatures, recovery processes not dependent on diffusion, such as cross slip are possible. The creep is still in the primary stage, however, because the strain hardening is not balanced out. Above about 0.5 $T_m$, significant diffusion increases the recovery processes, and steady state creep predominates. (22) With the homologous temperatures used in the present study, creep is not believed to ever have achieved the secondary stage.

Recrystallization. Recrystallization is a phenomenon which consists of the nucleation and growth of new, stress free grains in areas of high lattice strain energy, such as slip line intersections,

deformation twin intersections and grain boundaries.[23] The recrystallization process appears to be an important mechanism in many diffusion welding applications. In fact, Parks[24] concluded from his work with several different materials that recrystallization was the primary diffusion welding mechanism.

According to Parks[25], the mean yield strength of a material approaches zero during recrystallization. This would facilitate the crushing of asperities as discussed in the previous section, and promote intimate contact at the joint. For the application considered in the present study, the strain near the joint interface will result almost entirely from the crushing of surface asperities. In Parks study, the components were abraded by wire brushing or other means before assembly, with the intention of promoting recrystallization during the weld cycle. The delicate nature of the components in the Cassegrainian cell stack assembly would not permit such a pre-straining, and thus the total effect of recrystallization is expected to be lower in this application than in Parks' study.

Recrystallization may also be partly responsible for removing the contaminant layers from the joint interface.[26] When the base metal loses strength during

recrystallization, its support of the thin contamination film is momentarily released. The surface tension of the film then causes it to agglomerate, or ball up, leaving large areas of clean surface.

In addition, recrystallization can promote the atomic registry required for a sound bond. The growth of new grains can occur across the joint interface, often obscuring all traces of the bond line.

Of the many factors which influence recrystallization, the principal contributors are the temperature, the time at temperature, the degree of deformation and the purity of the material.[27] Grain size and crystal orientation also have noticeable effects, but are not considered pertinent to this study.

Recrystallization can normally be expressed by an equation of the form:[28]

$$1/\tau = Ae^{-Qr/RT}$$

where $1/\tau$ = the rate at which a certain percentage of the structure is recrystallized

$A$ = a constant

$T$ = annealing temperature

$R$ = the gas constant

and $Qr$ = the activation energy for recrystallization(9)

Because of the presence of a generally large activation energy in the above equation, recrystallization actually appears to occur at a definite minimum temperature. The temperature specified usually represents that which will result in complete recrystallization after 1 hour. A small decrease in temperature would require a significantly longer time for recrystallization, whereas an increase in temperature would sharply decrease the time required.

In general, recrystallization is promoted by increased amounts of previous cold work. In figure 7 are shown plots of the time-temperature relationships for the recrystallization of zirconium at two different degrees of cold work.[29] It is clear that a greater amount of cold work speeds the rate of recrystallization at a given annealing temperature.

The effects of impurity elements on the recrystallization of a metal depend on both the quantity and the type of solute. Extremely pure metals may have recrystallization temperatures at or below room temperature.[30] However, very slight impurity additions can drastically raise the recrystallization temperature.

Diffusion In addition to its effects on

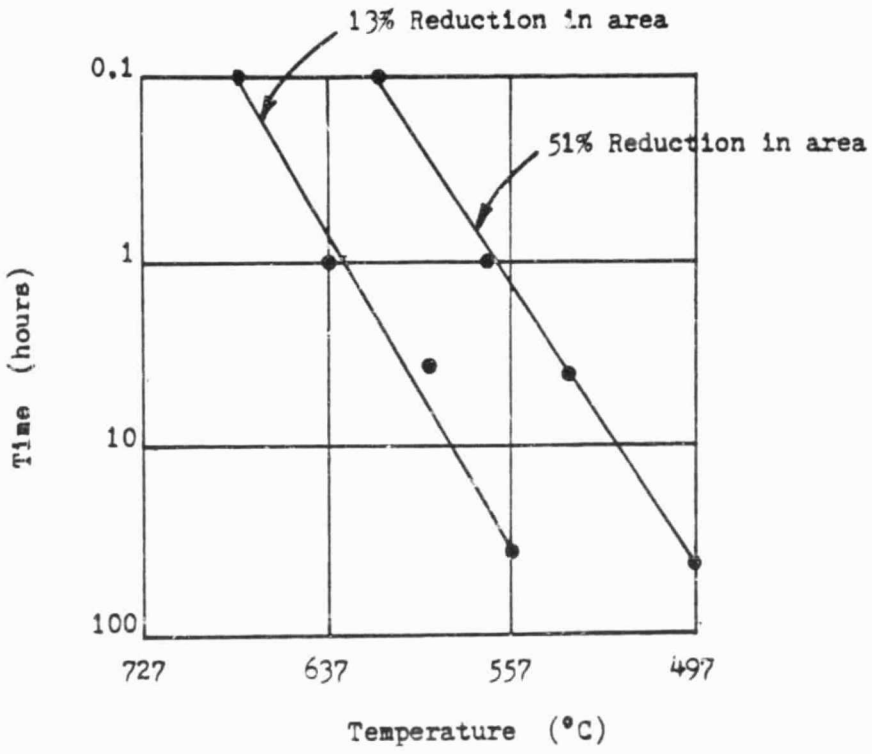


Figure 7: Time - Temperature relationships
for recrystallization of zirconium

recrystallization and creep, diffusion promotes bonding by the transport of contaminants and vacancies from the bond line to the surrounding base material. Although extensive diffusion would not be expected at the temperatures considered in this study, about 0.3 $T_m$, the distance and volume of diffusion need not be great to have an effect on welding.

The removal of contaminants from the bond line would be aided by their dissociation. Typical contamination consists of various organic and inorganic compounds, including the oxide layer. When these compounds dissociate under welding conditions, many of the elements released, such as oxygen, hydrogen and carbon, are small relative to metal atoms. Since they can occupy interstitial sites in the base metal, these elements diffuse rapidly from the bond line.

**Silver as a Diffusion Aid**

**Need for a Diffusion Aid.** The three materials constituting the present design of the cell stack assembly - GaAs, BeO, and Cu - have widely dissimilar properties. Joining together any such dissimilar materials would be difficult, but the problem is exacerbated by the natures of GaAs and BeO. The mechanisms for bonding discussed in the preceding section simply do not apply to these materials as they do to metallic materials. Fortunately, there exists a technique to simplify the situation which has met with considerable success in the past. The faying surfaces can be coated, either by vapor deposition or electroplating, with a material which has favorable properties for diffusion welding. Assuming that good adhesion of the layer to the substrate can be provided, the situation is resolved to the bonding of opposing surface coatings. For the present application, silver was chosen as the interlayer material for both joints.

**Reasons for Using Silver.** The choice of an interlayer material was simplified by the fact that the design already called for silver coatings on the parabolic mirror and the photovoltaic cell. By a fortunate coincidence, silver is one of the more easily

diffusion welded materials, because of its chemical nobility, plasticity, and low temperature of recrystallization.

Chemical nobility is a term which indicates that a metal resists the formation of compounds with other elements, especially oxygen. The resistance to oxidation can be quantified by a free energy of formation, the energy released when the compound is formed. A list of the free energy of formation of silver oxide ($Ag_2O$) with respect to temperature is displayed in table 1.[21] As shown, the quantity passes through zero at about 200 C and becomes more positive at higher temperatures. This indicates that the oxide would be more likely to dissociate than to form at temperatures above 200 C. Of the common metals, only gold has a less stable oxide.[32]

As is generally true for materials with a face centered cubic structure, silver exhibits excellent ductility. In tensile tests, fully annealed, 99.99% pure silver elongates about 50% before failure[33]. The yield strength has been observed to be as low as 1220 psi, but strain hardening raises the ultimate strength to 19,000 psi. The plasticity of silver would promote the initial stage of diffusion welding, wherein the contact area is

Table 1: Free Energy of Formation of $Ag_2O$

| Temperature ( F) | F (cal/mole) |
|---|---|
| 80 | -2500 |
| 300 | -650 |
| 400 | +200 |
| 500 | +1050 |
| 600 | +1900 |
| 700 | +2700 |

increased by microscopic plastic deformation.

As discussed in the preceeding section, recystallization is dependent on several factors, including temperature, degree of strain and material purity. In the case of silver, the onset of recrystallization in very pure, severely cold worked metal has been observed at room temperature. The concentrations of impurities in a typical commercially electroplated silver layer are listed in table 2.[34] Slightly strained silver of this purity would be expected to display a recrystallization temperature of about 200 C.[35]

**Previous Work on the Effect of Welding Conditions.** Several published studies have considered the diffusion welding of silver coated base materials. Those cases considered pertinent to this study are summarized in table 3. As shown, the base materials in all instances were metal alloys. Although the results of each investigation were considered to be satisfactory, the welding procedures and acceptance criteria vary widely. The joint requirements range from a 1000 psi burst strength for a cast aluminum body[36] to strengths approaching that of stainless steel in another study.[37] Factors varied in the welding procedures

Table 2: Impurity content of Silver Electroplate

| Element | Concentration (ppm) |
|---|---|
| Copper | 10 |
| Lead | 2 |
| Magnesium | 2 |
| Nickel | 4 |
| Iron | 8 |
| Oxygen | 23 |
| Nitrogen | 4 |
| Hydrogen | 5 |
| Carbon | 110 |
| Sulfur | 9 |

Table 3: Summary of Previous Work on Diffusion Welding Silver Coated Materials

| Investigators | Temp.'s Studied | Pressures Studied | Coating Method | Base Material | Environment | Coating Thickness | Surface Finish | Tensile Strength |
|---|---|---|---|---|---|---|---|---|
| Dini et.al. | 300,600 | 10,30 | Electro-plate | 304 SS Be | Flushed Ar | 1mil,6mil | 8-21μin RMS | 42-66 |
| Naimon et.al. | 204 | 17 | HHC PVD | 1100Al to 316 SS | not stated | 6 μm | lapped to .1μm | 47-50 |
| Crane et.al. | 260-370 | 25 | Electro-plate | 321 SS to 2219Al | Air | not stated | as rolled sheet | peel tested |
| Knowles et.al. | 107-343 | 10-30 | Electro-plate | Be,Mo,W 304 SS | Air | 200 μin | lapped to 20 μin | 22.5 |
| Morley et.al. | 482 | 3.84 | Electro-plate | Cast Al | Nitrogen | not stated | lapped | 8.27 |

Notes: HHC PVD - Hot Hollow Cathode Physical Vapor Deposition

All temperatures in °C

All pressures and tensile strengths in ksi

include surface preparation, coating technique, welding atmosphere and of course the parameters employed (time, temperature, pressure). It is apparent from the earlier discussion of welding mechanisms that all of these factors are intimately related. However, to promote the clarity of this discussion, the effects of these factors shall be considered separately.

Surface Preparation. The proper evaluation of the quality of a surface finish must include consideration of both roughness and flatness. Roughness is a small scale variation in the surface profile, and accounts for what has been referred to as asperities, the small "hills" on the surface. Flatness is the condition of the surface profile as considered over the entire area of the part. The difference between roughness and (lack of) flatness is illustrated in figure 8. A lack of flatness or "waviness" of a surface is a much more severe condition for diffusion welding than is roughness. Surface asperities may be eliminated by microscopic plastic deformation, recrystallization and creep as discussed earlier, but the amount of material redistribution required to provide intimate contact between wavy surfaces may be orders of magnitude greater. Even if the pressure and temperature used were great

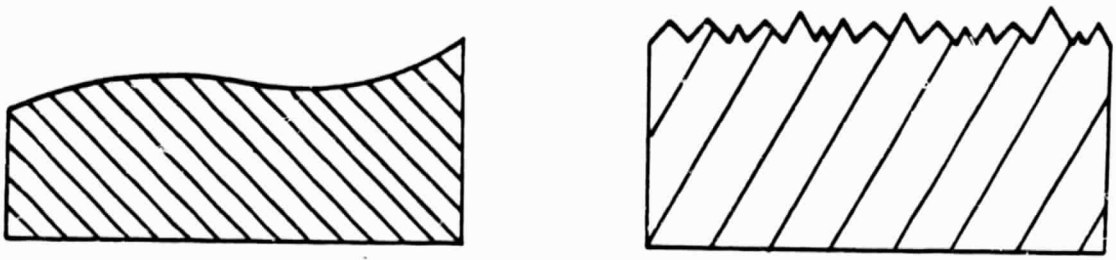

Wavy surface

Rough surface

Figure 8: Cross sectional views of typical surface irregularities.

enough to mate the surfaces, excessive distortion and/or cracking of the components would be likely to occur.

The most effective surface preparation technique employed in the published studies was lapping. As indicated in table 3, this method provided surfaces which were quite flat, to within 0.1 in. over a 0.5 in. sample in the best case.[38] Such careful surface preparation would be expected to lower the required temperature and pressure for a successful weld.

The disadvantage of lapping is that it is a difficult procedure which requires special equipment. Dini et.al.[39] achieved excellent bonds with a lathe prepared surface, while Crane et.al.[40] simply used as rolled sheet material. Cold rolling should provide a surface of good quality, but the flatness might easily be disturbed by cutting the sheet into weld coupons.

Coating Technique. There are three methods of applying coatings commonly used for diffusion welding: electroplating, physical vapor deposition, and hot hollow cathode-sputter evaporation. Of the three, hot hollow cathode sputtering is considered the most desirable, both in purity of the deposited layer and adhesion to the base material.[41,42] In fact, Naimon et.al.[43] credited the technique with enabling them to

decrease the welding temperature in their studies. The disadvantage of hot hollow cathode sputtering is that it is difficult to perform, and elaborate equipment is required.

Perhaps the least desirable coating method for diffusion welding is ordinary physical vapor deposition. The deposited layers usually exhibit poor adhesion to the substrate.[44] Generally, the only justification in applying this method is when the nature of the base material is not compatible with either of the other methods.

The most commonly used method for depositing diffusion welding coatings is electroplating, principally because the technique is well developed and the equipment is usually readily available. Adhesion of the deposit to the substrate is somewhere between that of the other two methods. Purity of the deposit can be a problem, especially when proprietary brightening additions are made.[45]

When selecting the appropriate interlayer thickness for diffusion welding, the primary consideration is the stress which will be required to deform the layer, both in compression and tension. Triaxial restraint of the base material on the coating

tends to improve the strength of the joint in service, but also makes it more difficult to obtain intimate contact during the welding cycle.[46] The effective restraint decreases as the interlayer thickness increases. Thus, the relationship of joint strength to interlayer thickness would resemble the curve of figure 9.[47]

The initial portion of the curve in figure 9, in which the relationship is almost linear, represents a region of increasing bond area caused by improved plastic flow during welding. The maximum strength occurs when increases in interlayer thickness provide no further improvement in weld area. Any further increase in thickness decreases joint strength by reducing the effect of triaxial restraint in service.

The actual point where the maximum joint strength will occur is difficult to determine analytically, because it will depend both on the materials involved and the quality of the substrate surface. The greater the roughness and waviness of the surfaces, the thicker the interlayer will need to be. The thickness for the present study was chosen to be 0.0004 in., which has proved effective in other studies.[48,49,50] The scope of the study did not permit the thickness to be varied,

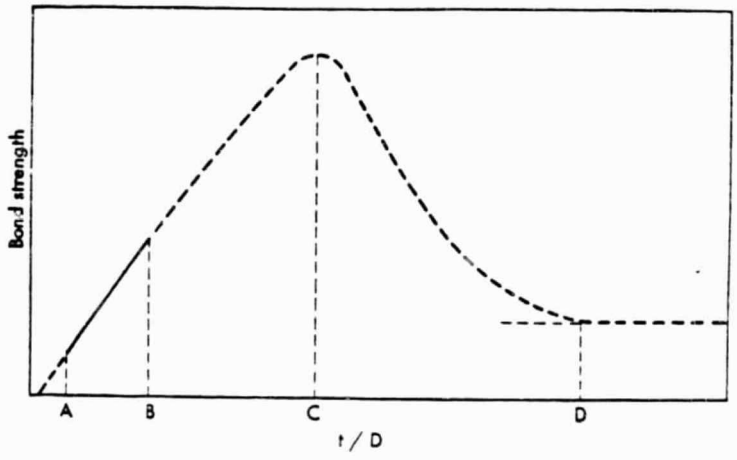


Figure 9: Relationship between joint strength and interlayer thickness.

and this should be considered for future work. However, it must be considered that with the available techniques, greater thicknesses tend to increase the waviness of the coating itself, regardless of the quality of the substrate surface.

Welding Atmosphere. When diffusion welding many materials, the welding atmosphere is critical and must consist of either a vacuum or a continuously flushed inert gas. With silver coated surfaces, however, the atmosphere has virtually no effect on weld quality.[53,54] Apparently, the welding atmosphere is only critical for materials which readily form compounds with elements in the air.

Crane et.al.[53] conducted welds in air with satisfactory results at all parameter combinations studied. Knowles and Hazlett[54] went further and compared the results of welds made in vacuum and in air at similar welding parameters. No effect of the atmosphere on joint quality was observed.

Temperature and Pressure. Low welding temperature and pressure are desirable for the present application to avoid damage to the delicate components involved. This presents a complication not encountered in most of the published studies. In cases where low welding

temperatures were sought, the applied pressure was generally high to compensate.

Naimon et.al.[55] used a temperature of only 204 C to join aluminum to stainless steel with a silver interlayer, but the pressure of 16,969 psi was sufficient to cause extensive plastic deformation of the aluminum component. Similar methods were used by Crane et.al.[56] for bonding aluminum to stainless steel. The temperatures used ranged from 260 to 370 C with a pressure of 25,000 psi. Dini et.al.[57] achieved high joint strength in stainless steel at 300 C and 10,000 psi, but these were the lowest parameters considered. An important aspect of their results is illustrated in figure 10. As indicated, the pressure was much more significant at low temperatures than at high temperatures.

A rather atypical study was that performed by Morley and Caruso[58]. Silver electroplated, cast aluminum valve bodies were welded in that study. A relatively high temperature of 482 C was used with a low pressure of 3,840 psi. A respectable tensile strength of 8,270 was achieved.

Only two published studies could be located in which both low temperatures and low pressures were

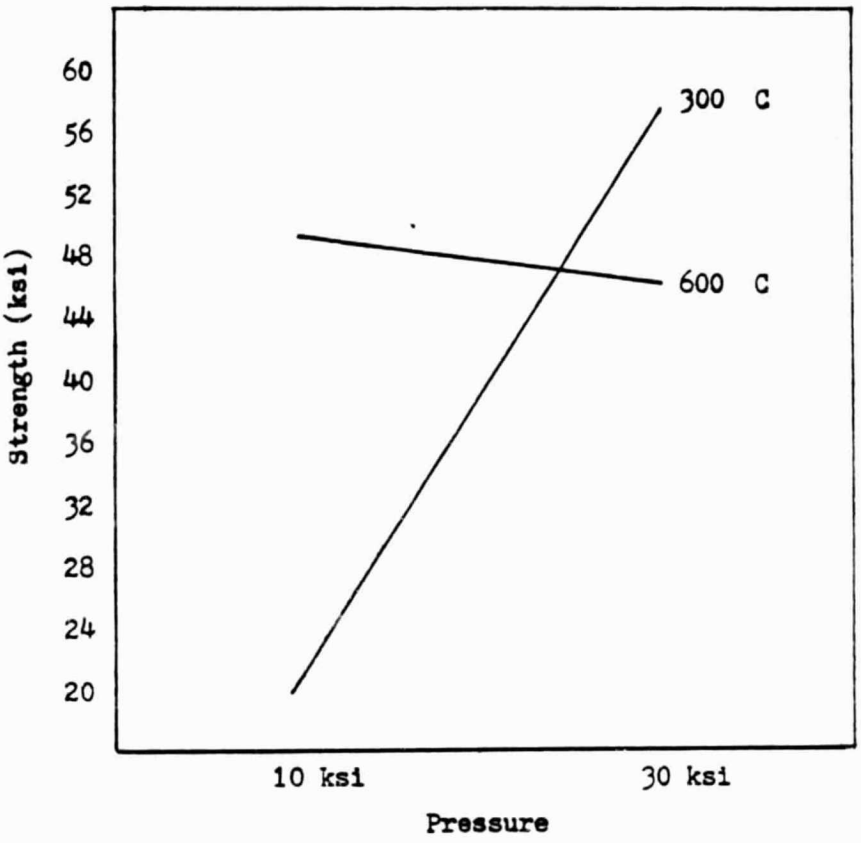


Figure 10: Joint strength vs. welding pressure, from the work of Dini et. al.

considered. O'Brien et.al.[59] welded maraging stainless steel coupons which had been coated with silver by the hot hollow cathode sputter-evaporation process. The samples were polished flat to within one light band before coating. The results are shown in figures 11 and 12. The samples represented by the curve of figure 11 were welded at 204 C. It appears that above about 10,000 psi, no significant increase in strength was achieved with further increase in pressure. Below 10,000 psi the strength rapidly decreased with lower pressure, although the joints formed at 5000 psi still maintained some strength. The curve of figure 12 represents the results of maintaining a constant pressure of 20,000 psi and varying the temperature. It is interesting to note that a change in slope appeared to occur around 200 to 300 C, because within this temperature range recrystallization and the dissociation of AgO are expected to begin.

Knowles and Hazlett[60] also considered low temperatures and pressures in the bonding of silver electroplated beryllium. Before plating, the samples were lapped flat to within 20 in. over a 0.5 in. diameter area. The results of the study are displayed in figure 13. A significant increase in strength was apparent over the

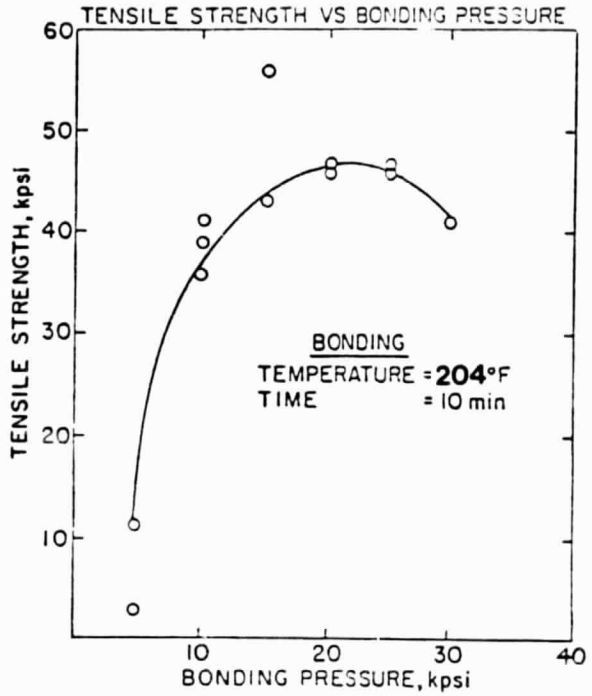


**Figure 11: Joint strength vs. welding pressure from the work of O'Brien et.al.**

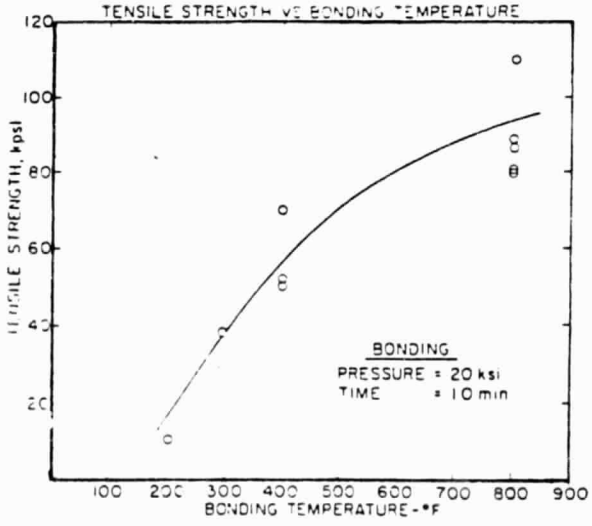


**Figure 12: Joint strength vs. welding temperature from the work of O'Brien et.al.**

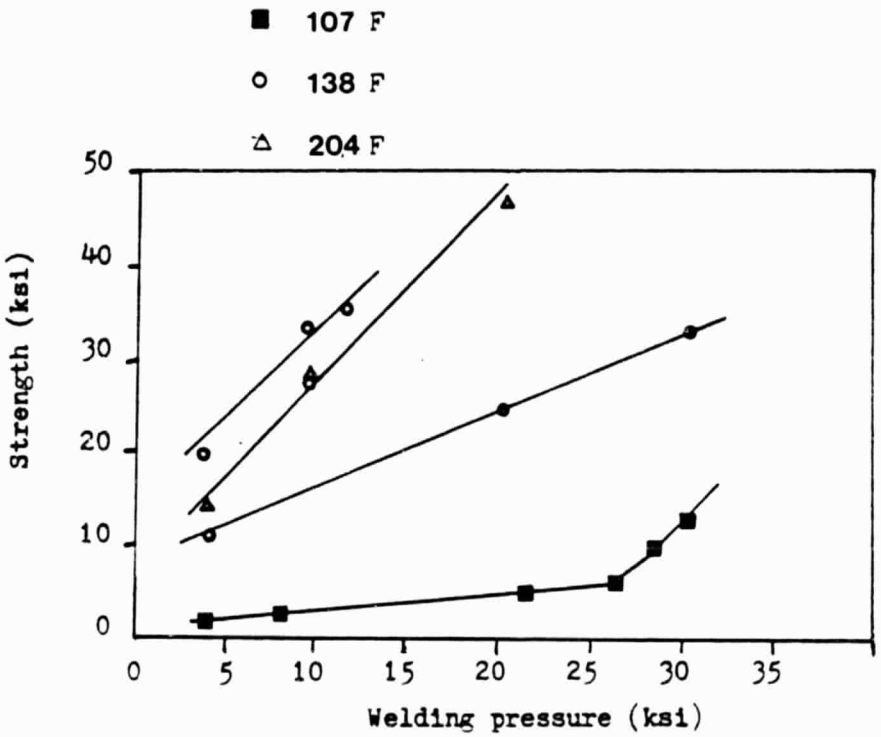


Figure 13: Joint strength vs. welding pressure, from the work of Knowles and Hazlett.

entire pressure range when the temperature was increased from 225 to 280 C. The sharp decrease in strength at pressures below 10,000 psi observed by O'Brien et.al. was not apparent in Knowles and Hazlett's data. Rather, the relationship between welding pressure and the resulting joint strength seemed roughly linear.

Time. Although diffusion is a time related process, the typical conclusion of published studies is that time at temperature is a relatively insignificant factor in diffusion welding.[61,62,63] Investigators welding silver coated materials have varied time at temperature from one minute to several hours, without an appreciable change in resulting joint strength.

Apparently, the kinetics of diffusion welding are relatively fast, even at the lower end of the useable temperature range. The effect of time is usually obscured, however, by the low heating and cooling rates used to prevent damage from thermal shock. This would add appreciably to the effective time at elevated temperature.

**Diffusion Welding Pressure Systems**

There are two basic families of pressure systems generally used for diffusion welding: uniaxial and isostatic. The former is by far the more popular type, and was used in all of the published studies on diffusion welding silver coated materials. The latter type is more complex and often more expensive, but it has characteristics which make it more suitable for certain difficult applications.

**Uniaxial Pressure Systems**. The popularity of uniaxial pressure systems results from the fact that they are relatively easy to construct and operate. Such systems are distinguished by the fact that they exert pressure in one direction only. Pressure application generally depends on either differential thermal expansion or a hydraulically operated piston.

A differential thermal expansion setup is extremely simple, but the pressure cannot be controlled independently of the temperature. With hydraulically actuated systems, the pressure can be controlled without regard to the temperature, and yet the system's design remains relatively uncomplicated. The basic limitation of uniaxial systems arises from the difficulty in providing adequate alignment of the

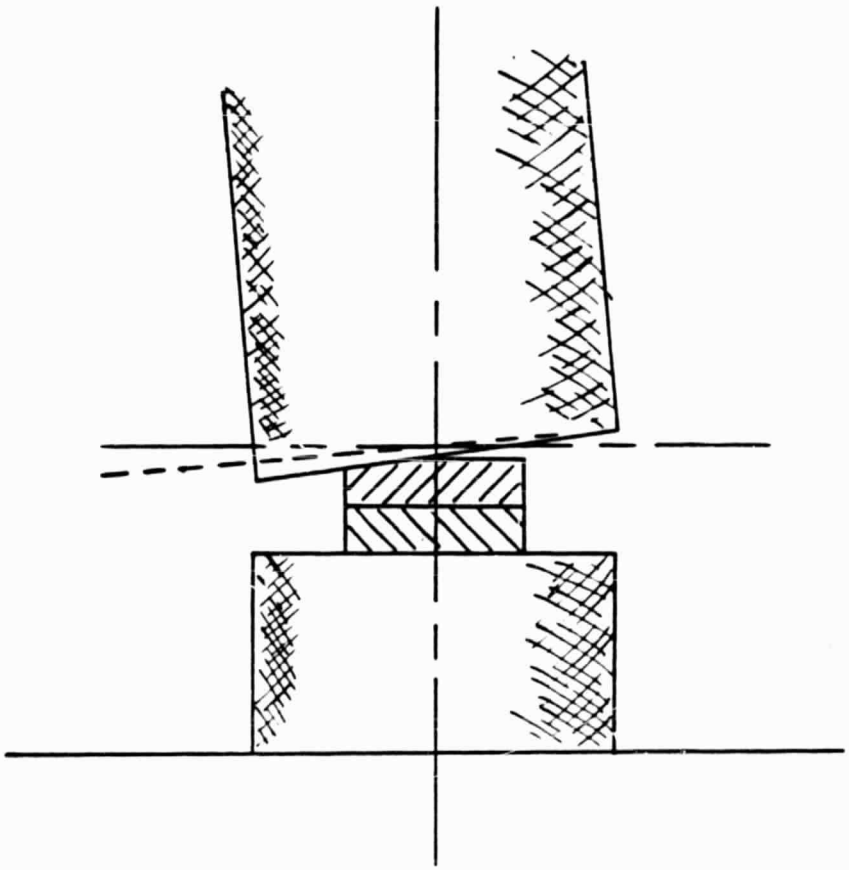

Figure 14: Misalignment problem in a uniaxial pressure system.

piston, the anvil and the joint components. Unless the contacting surfaces of all of the members are completely flat and parallel to one another, the application of pressure will be uneven. As shown exaggerated in figure 14, misalignment results in contact over a relatively small area where the welding force is concentrated. Thus welding tends to be incomplete, and distortion or cracking of the components is likely.

**Isostatic Pressure Systems**. By far the most common isostatic pressure system used for diffusion welding is the hot isostatic press (HIP). HIP units have also been used extensively for powder metal compaction and healing of internal voids in castings.[64] A schematic diagram of a typical HIP unit is shown in figure 15. The system is basically a pressure vessel with an internal, removable thermal barrier package which prevents the pressure vessel walls from being heated. Heating is provided by resistive elements, and the temperature is monitored by thermocouples. The vessel is evacuated and back-filled with argon gas which, when compressed by a hydraulic pump, can provide pressures near 30,000 psi.

The weld assemblies must be placed in a sealed container so that the argon gas will not seep into the joints. The containers are designed to collapse evenly

around the assemblies when pressure is applied. Aside from the slight pressure increase which will occur when the container collapses around the assemblies, the internal atmosphere will remain at essentially ambient pressure. A pressure differential will thus exist between the inside and outside of the container, which is necessary to press the joint components together.

It is critical that the container collapses evenly around the joint components so that isostatic pressure is maintained. Care must therefore be taken in choosing the container's dimensions and material. It is desirable that empty spaces within the container be minimized, to minimize the amount the container must collapse. For many applications this is difficult to accomplish because the assemblies are irregular or very small. In such cases a fine granular material is poured into the container to fill the voids.

Choosing the granular pressure transfer medium also requires careful consideration. The material used must flow almost like a liquid to preserve the isostatic nature of the pressure. This is generally the most difficult requirement to satisfy because under welding conditions most materials tend to clot together to a certain extent. In addition, the material must display

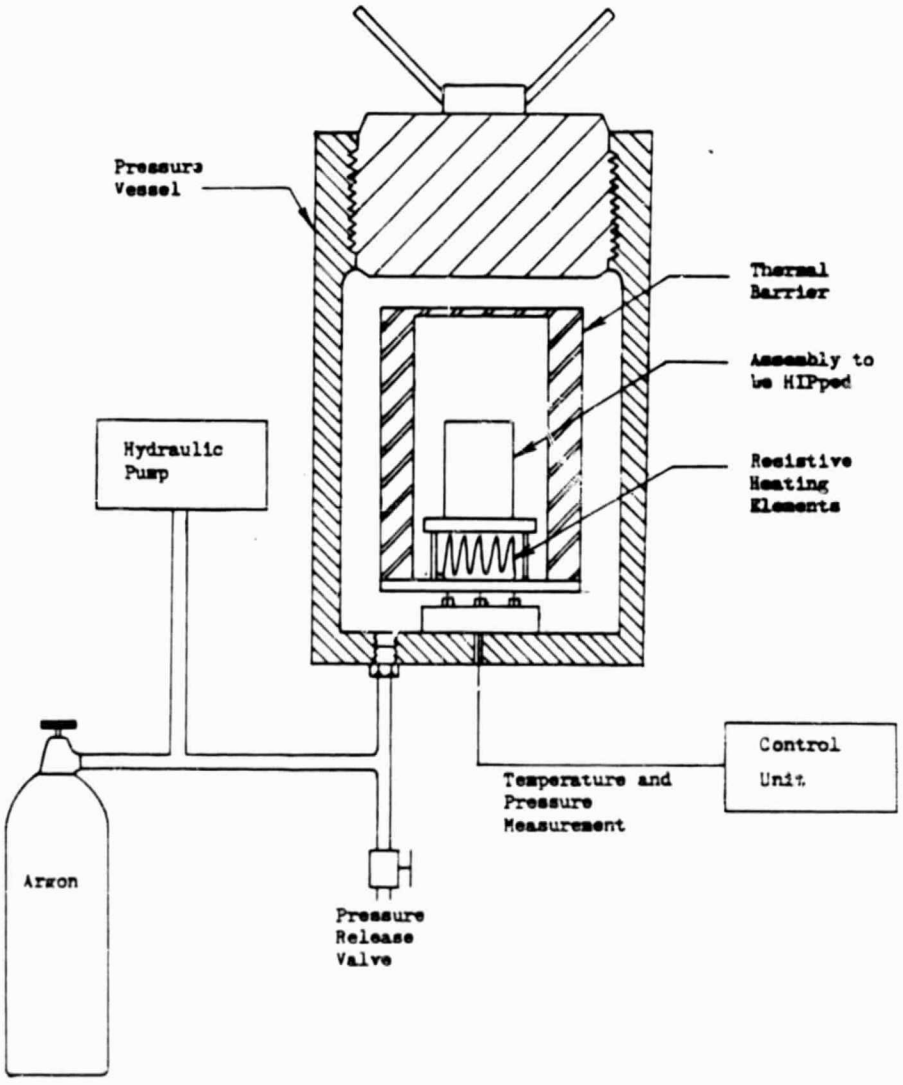


Figure 15: Schematic diagram of HIP Unit

good thermal conductivity, and should be relatively inert to prevent interaction with the joint components.

Despite the complications involved in isostatic systems, the advantages afforded occasionally make it worthwhile. The greatest advantage is the even pressure application provided, especially when using a granular pressure medium. A granular material will easily mold around complex shapes with great accuracy. With true isostatic pressure on the components, macroscopic deformation can be avoided even at pressures above the yield strength, because the shear stress will be zero, as indicated by the Mohr's circle equation for state of stress[65]:

$$\tau_{max} = (\sigma_x - \sigma_y)/2 + \tau_{xy}^2$$
$$= (P-P)/2 + 0$$
$$= 0$$

where $\tau_{max}$ = maximum shear stress
$\sigma_x$ = normal stress in x direction
$\sigma_y$ = normal stress in y direction
$\tau_{xy}$ = shear stress in x plans, y direction
and P = applied pressure

Finally, the dense argon gas provides an excellent thermal transfer medium, resulting in very even heating of the assemblies.

**Conclusions**

After a review of the available literature, several conclusions may be formed concerning the diffusion welding of silver coated materials:

1) The principal mechanisms for diffusion welding are macroscopic plastic deformation, creep, recrystallization and diffusion of contaminants into the base material.

2) Coating the surfaces with silver promotes welding because of silver's plasticity, chemical nobility and low temperature of recrystallization.

3) Previous work demonstrates that welding silver coated surfaces in air has no deleterious effect.

4) Only two investigations considered the welding of silver coated materials at both low temperature and low pressure, as is of interest to this study. An expansion of the data base is therefore required.

5) There are two basic families of pressure systems useful for diffusion welding, uniaxial and isostatic. The former type is applicable to an introductory study only, as its limitations

make it unacceptable for welding the brittle components of the actual assemblies. The isostatic type of system is more complex, but better suited to welding brittle materials.

## OBJECTIVES

The ultimate purpose of the present study was to develop a satisfactory joining preocedure for the Cassegrainian concentrator cell stack assembly. The available time and funding did not permit a comprehensive investigation, with comparison of different processes. Diffusion welding was singled out as the most promising method, and was used for all of the experimentation.

An extensive literature search revealed the necessity of coating the joint components with silver, and a shortage of data relating strength to welding parameters in the range of interest. The first objective of this investigation was thus to further develop an understanding of the relationship between welding temperature and pressure and the resulting joint strength.

The brittleness of gallium arsenide, the photovoltaic cell material, made it clear from the onset that cracking would be a significant problem. Therefore, the second major objective of this study was to investigate the cracking problem as it relates to welding parameters.

## EXPERIMENTAL PROCEDURE

### Plan of Investigation

The data presented in chapter 2 from published studies on the diffusion welding of silver coated materials were considered to be insufficient for this study. The low temperatures and pressures necessary to avoid damage to cell stack components were considered in only two of the investigations, and those employed elaborate surface preparation techniques which would influence the results. In addition, although the results were not entirely contradictory, neither were they entirely consistent, and a more certain knowledge of the process was needed for the present application. Thus, it was necessary to expand the data base relating welding parameters to the resulting joint strength.

The actual cell stack components are expensive, and their brittleness and small dimensions preclude much quantitative mechanical testing. Therefore, it was not feasible to develop a large data base with the actual assemblies. Previous work showed that the base material has little or no effect on the variation in strength with changing welding parameters, although the absolute strength is affected.[21,23] For the initial investigation, silver electroplated steel coupons were

welded with a uniaxial pressure system. Steel was chosen because it is strong, ductile, inexpensive and relatively easy to electroplate. The uniaxial pressure system was used because it was much more economical for evaluating a large number of parameter combinations rather than an isostatic system.

Temperatures and pressures outside the usable range predicted for the cell stack components were studied in order to observe the strength loss which occurs at lower values of temperature and pressure. It would have been advantageous to have used pressures even lower than the minimum studied, but the servo control of the Gleeble ( the pressure system used in this phase of the study) was not accurate at very low levels of force.

In the second phase of the investigation, mockups of the actual cell stack assembly were welded using a hot isostatic press (HIP). Because of the expense of using the HIP, only a limited number of runs could be performed. The GaAs and BeO components were used as received from the suppliers, since available methods of further polishing did not hold much promise for improving the finish. The cold rolled Kovar sheet was also used as received, because the finish appeared quite good. The finish on the Cu components might have been

improved by further polishing, but this was not considered necessary because of copper's excellent ductility and low yield strength.

The investigation concentrated on three important subjects, which overlapped in the testing to some extent:

1) Developing a satisfactory encapsulation procedure for the assemblies.
2) Studying the effects of welding temperature, pressure, time and cooling rate on the resulting bond quality.
3) Studying the effects of the above parameters on cracking in the GaAS.

The first phase of the investigation and the initial HIP runs gave a good indication of which parameters would provide good bonding. The remainder of the HIP runs were therefore concerned with studying the cracking problem in the GaAs. The low pressures used were not expected to provide 100% bonding over the joint surface, but it was hoped that the tests would provide an insight into the causes of the cracking problem, and lead to recommendations for reducing the problem. Further, it is not expected that 100% bonding is necessary to provide the thermal fatigue resistance

required for the intended application.

**Special Equipment and Materials**

A photograph of the uniaxial system used for the first phase of the investigation is shown in figure 16. The system, called a Gleeble, consists of the control panel and a micro-computer at (the left of the photograph), and the thermo-mechanical unit (at the right of the photograph). The weld samples were held between 0.5 in. diameter class 2 copper electrodes machined to a 0.250 in. diameter at the ends. The electrodes were threaded into water cooled copper jaws, through which electric current was passed. The right hand jaw is fixed, while the left had jaw, attached to a piston, is free to move. Force is exerted by a hydraulic system acting on the piston.

A schematic of the Gleeble is displayed in figure 17. Temperature is monitored by 0.005 in. diameter Chromel-Alumel type thermocouple wires percussion welded to one joint component. The pressure is measured by a load cell. Both signals are sent to a microprocessor which effects the control. The desired thermal history is provided by resistive heating of the joint components. Deviations from the program are corrected by altering the current flow. The accuracy of the

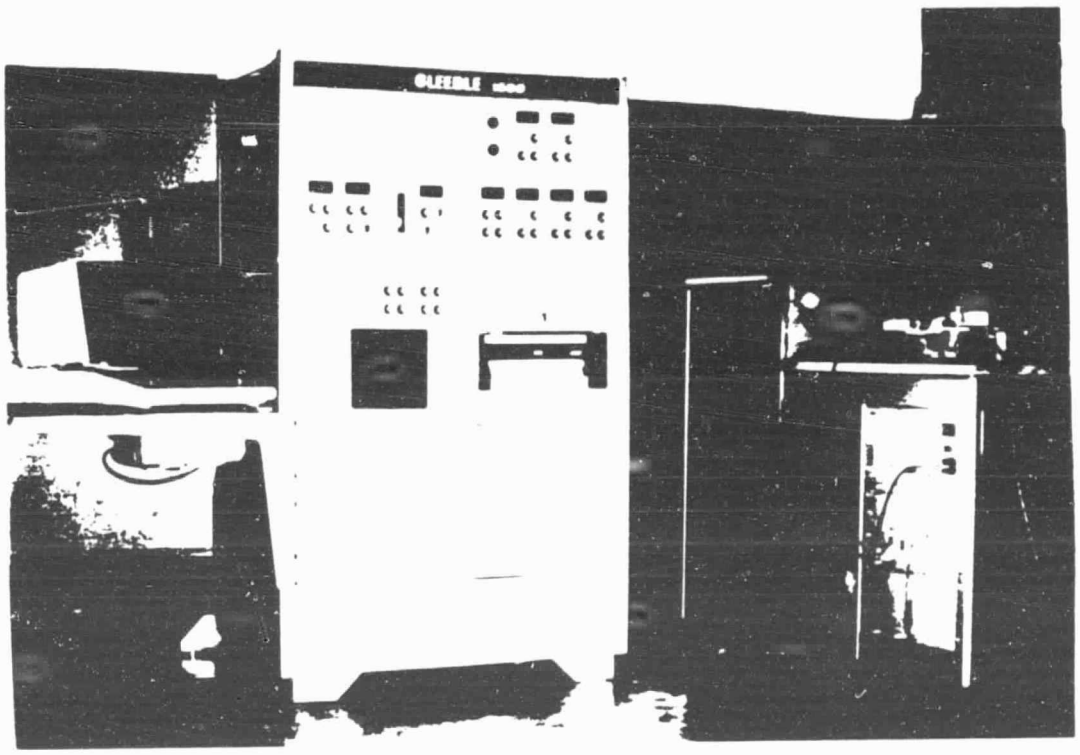

Figure 16: Photograph of Gleeble used in first phase of the investigation.

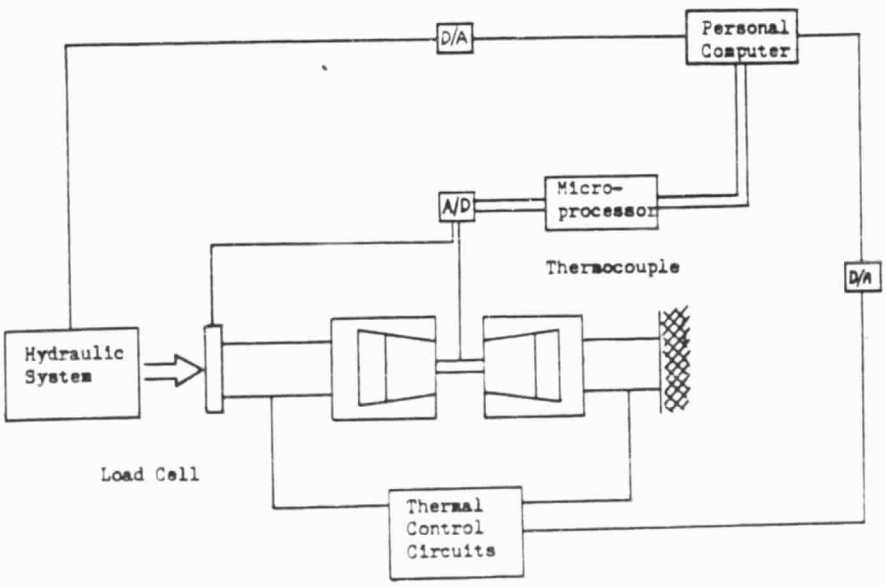


Figure 17: Schematic diagram of Gleeble.

temperature control is approximately ±5 C. Control of the welding force is estimated to be within ±20 lb.

The HIP unit is discussed to some extent in chapter 2. The system used, shown in the photograph of figure 18, is owned by Conaway, Inc. of Dublin, Ohio. The control console to the right of the photograph contains a stripchart recorder, a digital display of pressure and temperature and a dial for adjusting the temperature. The unit to the left of the photograph contains the pressure vessel, the hydraulics and the thermal electrical circuits. The system's automatic control is not functional, so the parameters were controlled manually from the digital display. The manual control is accurate to within ± 10 C for the temperature and -0, +250 psi for the pressure.

The silver coated GaAs components were obtained by NASA through Advanced Solar Energy Concepts of California. The silver coating appeared to have been applied by vapor deposition, and was evaluated as being generally rather poor in quality. The silver coated BeO chips were purchased from the Brush Wellman Co., of Cleveland, Ohio. The parts were ground flat to within 0.0002 in before applying the coating. The coating consisted of a thick film conductive medium (molybdenum

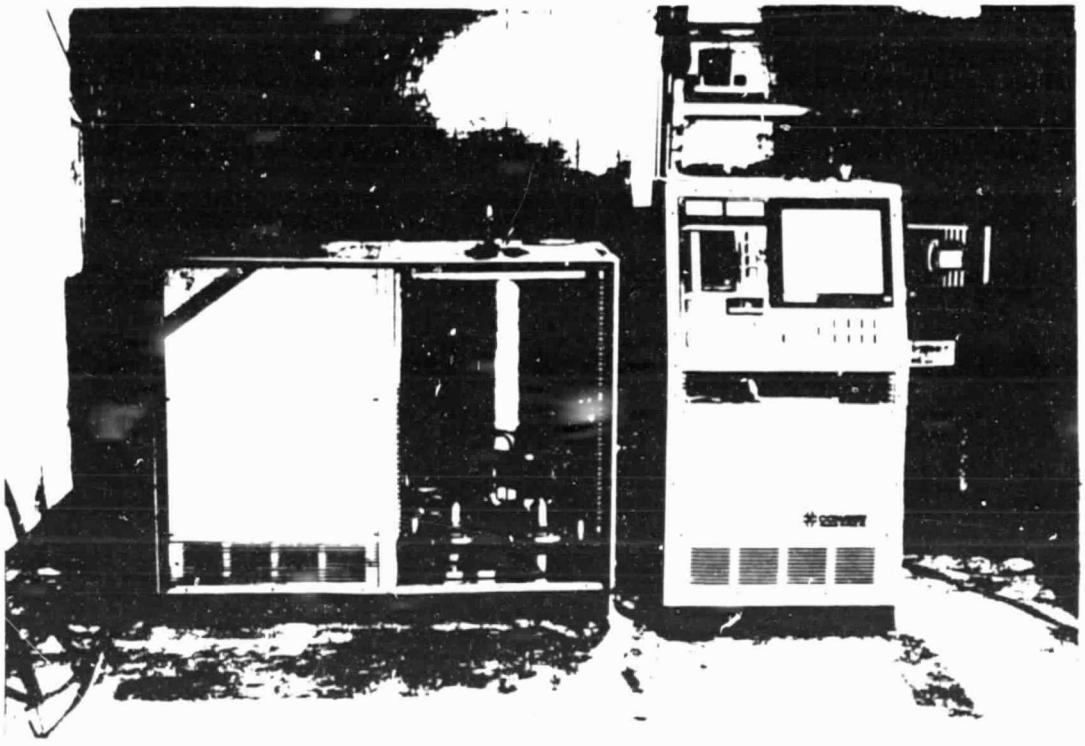

Figure 18: Photograph of Hot Isostatic Press used in second phase of the investigation.

and manganese) covered by 0.0002 in. of silver.

**Experimental Procedure**

Gleeble Study. Sample preparation consisted of the following procedure:

1) Mild steel sheet, 0.040 in. thick, was sheared into pieces 10.5 x 2.5 in.
2) A 5/8 in. wide strip was polished on the 10.5 in. side using grit paper bonded to a flat, machined steel block. Grits 240,320,400 and 600 were used.
3) The polished parts were sent to the Bron Shoe Co. of Columbus, Ohio for silver electroplating. A nickel strike and conventional techniques were employed.
4) The plated sheets were sheared into 5/8 x 2.5 in. coupons.
5) The coupons were clamped in a vise in pairs with a 5/8 in. square area of overlap. A 0.062 in. diameter hole was drilled through the edge to a depth of 3/16 in. The finished parts were as shown in figure 19.
6) The chromel-alumel thermocouple wires were bonded simultaneously to the bottom of the groove on one of the joint components, as shown

in figure 20.

7) A ceramic insulator tube was threaded onto the thermocouple wires to keep them separated.

The cleaning procedure for the joint components consisted of the following:

1) The samples were ultrasonically cleaned in trichloroethylene for a minimum of 10 minutes.

2) The parts were rinsed in acetone, distilled water and methanol, and then dried with a hot air blower.

The welding procedure consisted of the following:

1) The components were positioned between the copper electrodes as shown in figure 21.

2) A typical weld program is shown in figure 22. The pressure was raised to the weld level in 10 seconds, followed by a 5 minute ramp of temperature to the weld level. Pressure and temperature were then held constant for 10 minutes. The joint was cooled to room temperature in 15 minutes, and the pressure was then released.

HIP Study. Sample preparation consisted of the following procedures:

1) Kovar sheet, 0.015 in. thick, was sent as

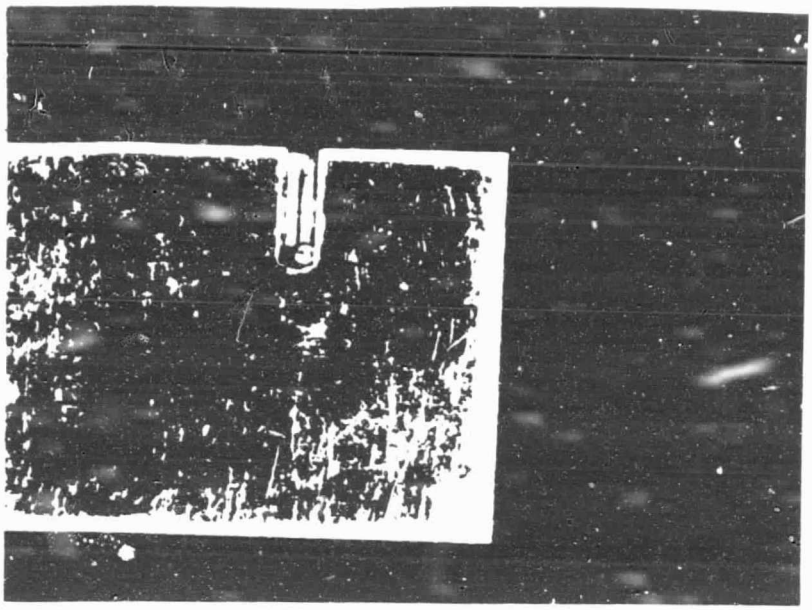

Figure 19: Electroplated steel coupon with 0.062" diameter notch.

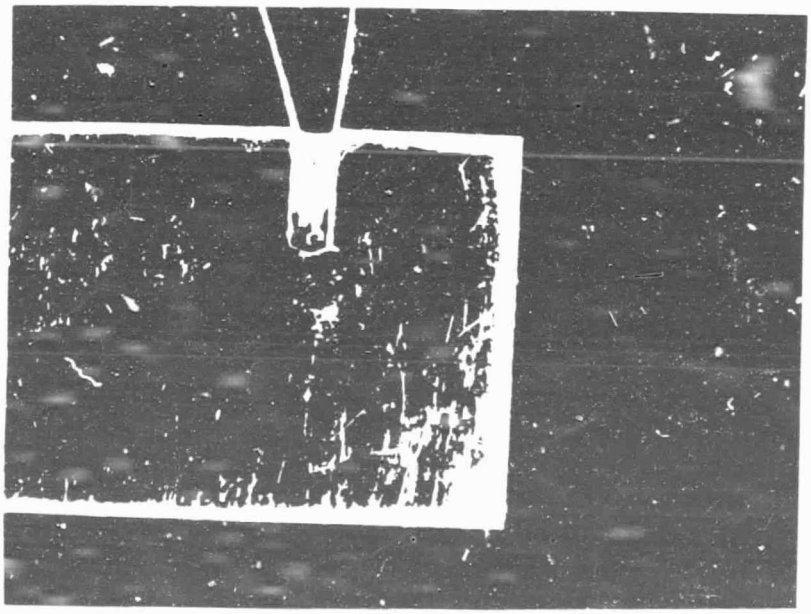

Figure 20: Steel coupon with thermocouple wires attached.

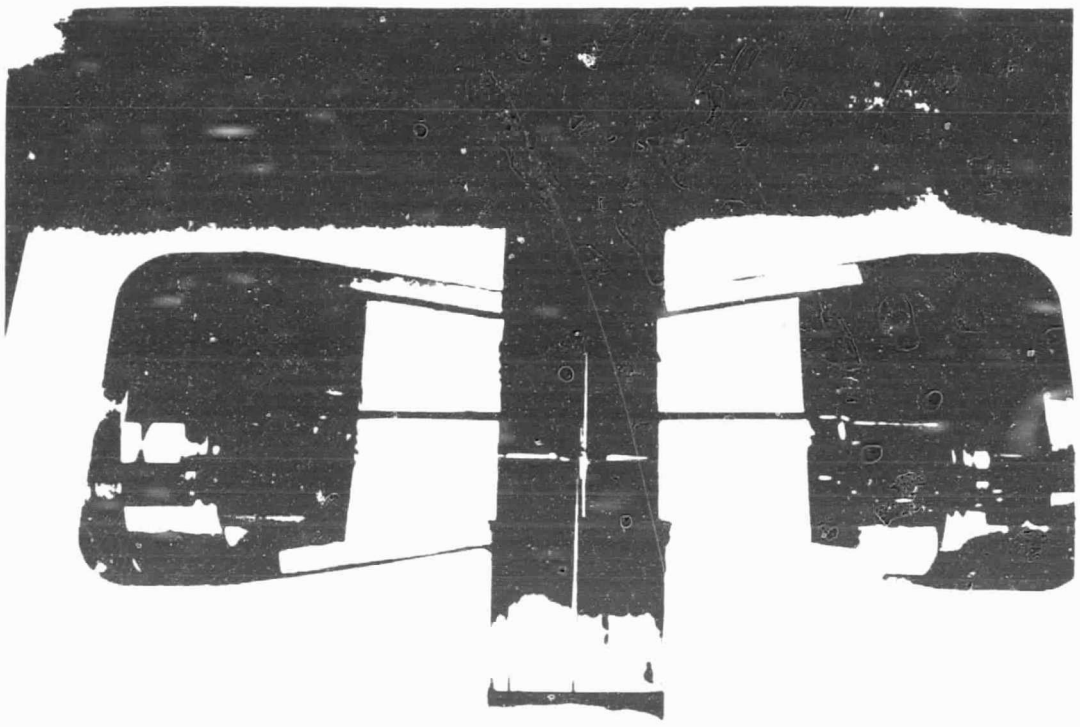

Figure 21: Photograph of Steel coupons clamped between the Gleeble's jaws.

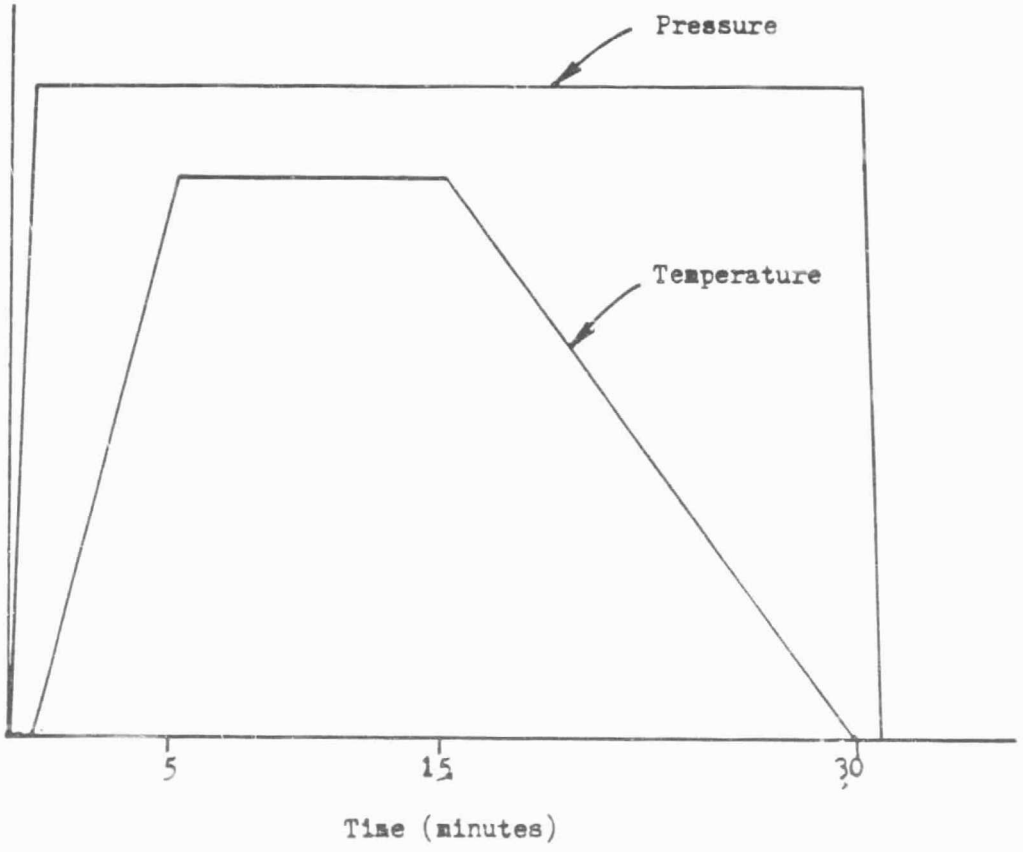


Figure 22: Typical Gleeble weld program.

received to Smith Electrochemical Co. of Cincinatti, Ohio for electroplating with 0.0002 in. of Ag.

2) The plated Kovar sheet was sheared into squares 8 mm. on a side.

3) A copper sheet, 10.5 x 2.5 x 0.015 in. was polished with grit paper bonded to a flat, machined block. Grits 240, 320, 400 and 600 were used.

4) The Cu sheet was sent to the Bron Shoe Co. of Columbus, Ohio for electroplating with 0.0002 in. of Ag.

5) The plated Cu sheet was sheared into squares 11 mm on a side.

The cleaning procedure for the BeO, Kovar and Cu components was as follows:

1) Ultrasonic cleaning in trichloroethylene, acetone and distilled water for 3 minutes each.

2) Rinse in methanol followed by blow dry with a hot air blower.

Ultrasonic cleaning tended to cause cracking in the GaAs components. Therefore, an alternate procedure was developed as follows:

1) The components were hand polished on nap cloth

using a slurry of 0.05 m. alumina powder in distilled water.

2) The components were rinsed in acetone, distilled water and methanol and then dried with a hot air blower.

After cleaning, the assemblies were visually aligned and wrapped in aluminum foil, as shown in figures 23 through 26. The hand wrapped aluminum layer served to hold the assemblies in alignment during handling, and also kept the granular pressure transfer medium from penetrating the joints.

The encapsulation procedure evolved over the course of the first few HIP runs. For the first two runs, deep drawn cans were used, of the dimensions shown in figure 27. Also shown in figure 27 is the manner in which the assemblies were placed in the cans. Granular graphite was used as a pressure transfer medium. For the first run, only one steel can was used, packed with 6 assemblies. For the second run, four cans were used, two steel and two aluminum. The steel cans were autogenous GTA welded shut, while the aluminum cans were sealed with a $CO_2$ laser. One of the steel cans had a 3 in. long, 0.25 in. O.D. copper tube brazed into a hole in the center of the lid. The tube was used to evacuate the

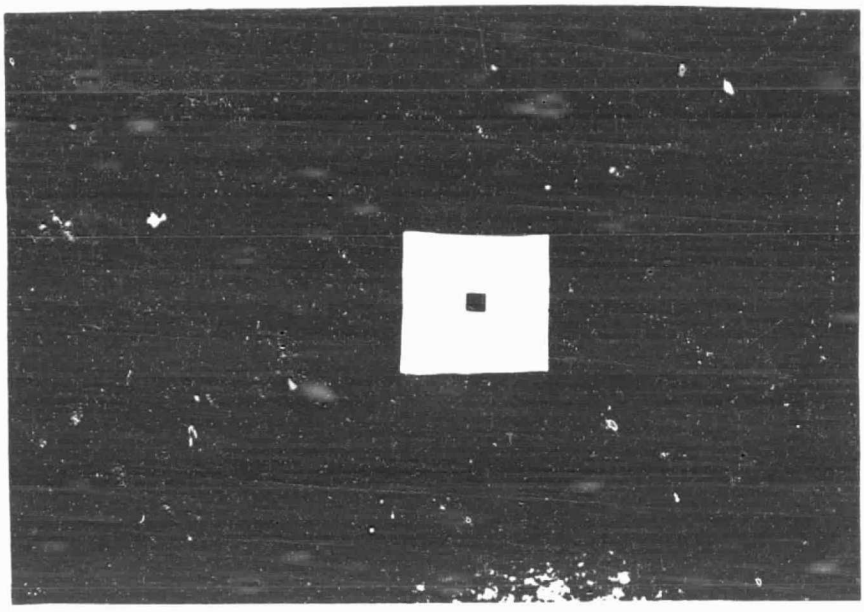

Figure 23: Assembly components aligned on aluminum foil.

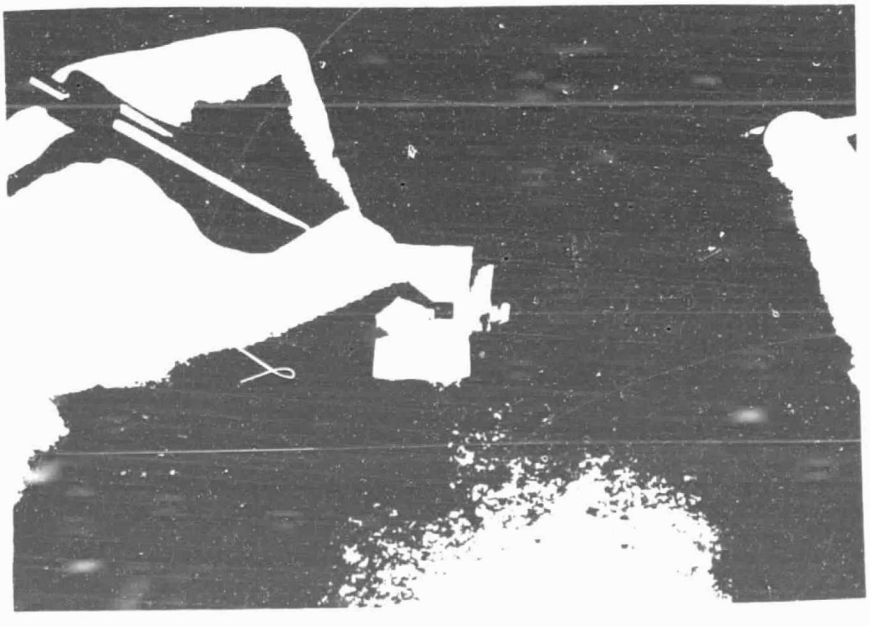

Figure 24: Components held in place with a graphite pencil as foil folded over.

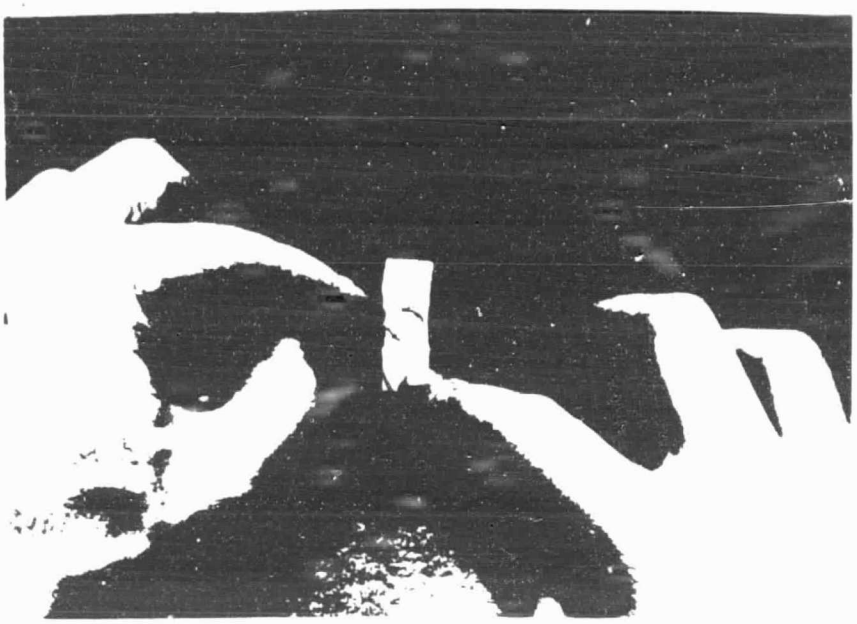

Figure 25: Aluminum foil wrapped around assembly.

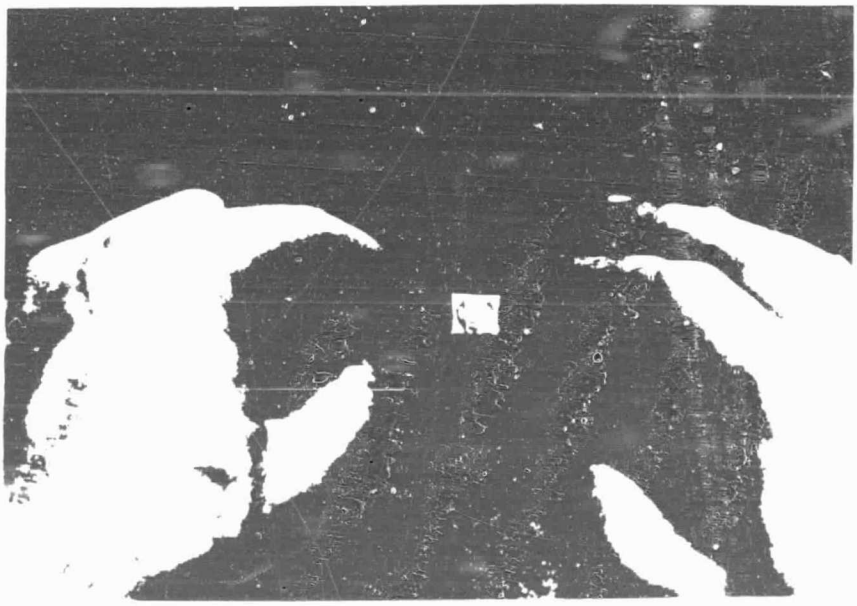

Figure 26: Complete, wrapped assembly

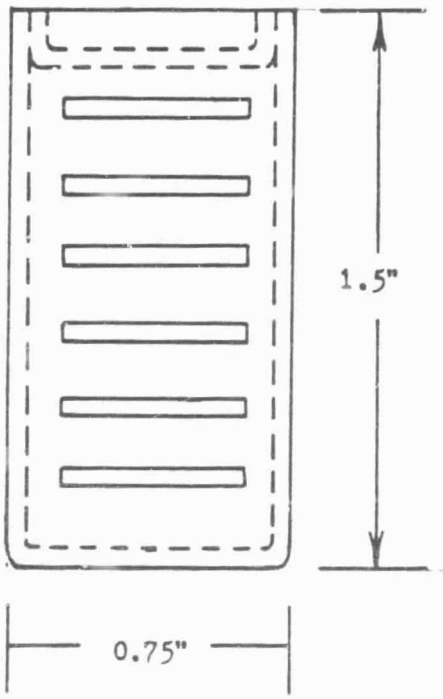


Figure 27: Deep drawn container used in initial HIP runs.

Deep Drawn
Container

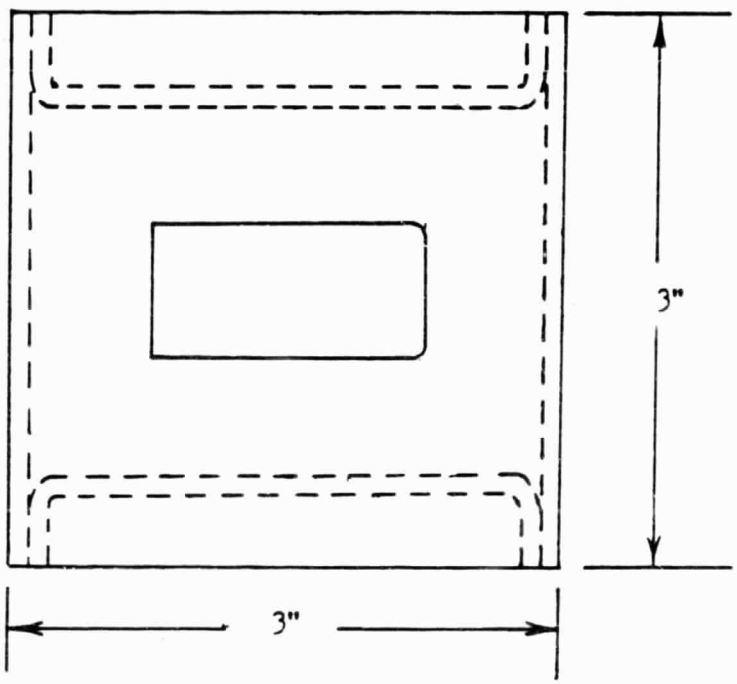


Figure 28: Larger container used in later HIP runs.

can and was then pinch welded shut with a crimping tool.

For the third HIP run, 6 assemblies were packed in 2 aluminum cans as above. The aluminum cans were then packed in a larger mild steel can as shown in figure 28. The pressure transfer medium in the smaller cans was granular graphite, while the larger can was packed with a fine, crystalline quartz. The large steel can was fabricated from a section of thin walled pipe and 2 "dished" lids. The upper lid had a short section of 0.25 in. diameter steel tubing GTA welded in its center.

The remainder of the HIP runs used the steel can only. The final procedure is depicted in figures 29 through 32. The lower lid was first GTA welded to the section of pipe. Granular graphite was then poured in and tamped down to a depth of 0.5 in. Three assemblies were positioned in the can as shown in figure 30. A steel disk, polished flat on both sides was placed over each of the assemblies, and another assembly was placed on top, as shown in figure 31. The remaining volume of the can was then filled with granular graphite which was tamped down using a lid. The upper lid, with a short tube welded in its center, was then GTA welded on. The end of the tube was also sealed by GTA welding. The finished can was as shown in figure 32. Variations in the

Figure 29: Components of HIP Container.

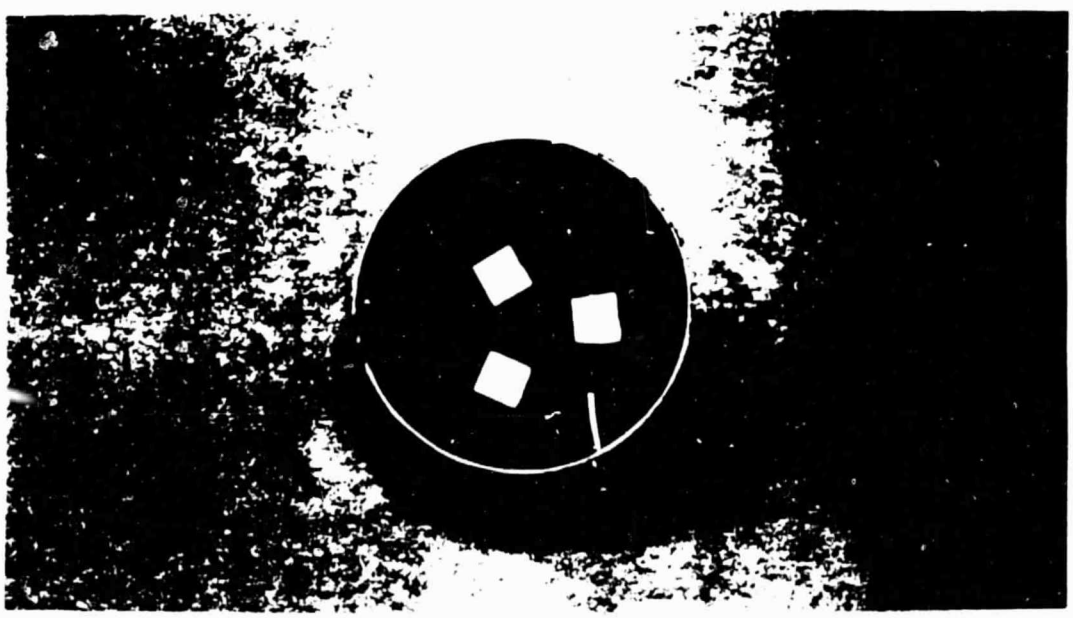

Figure 30: Granular graphite poured in to a level of 0.5", and three assemblies placed on top.

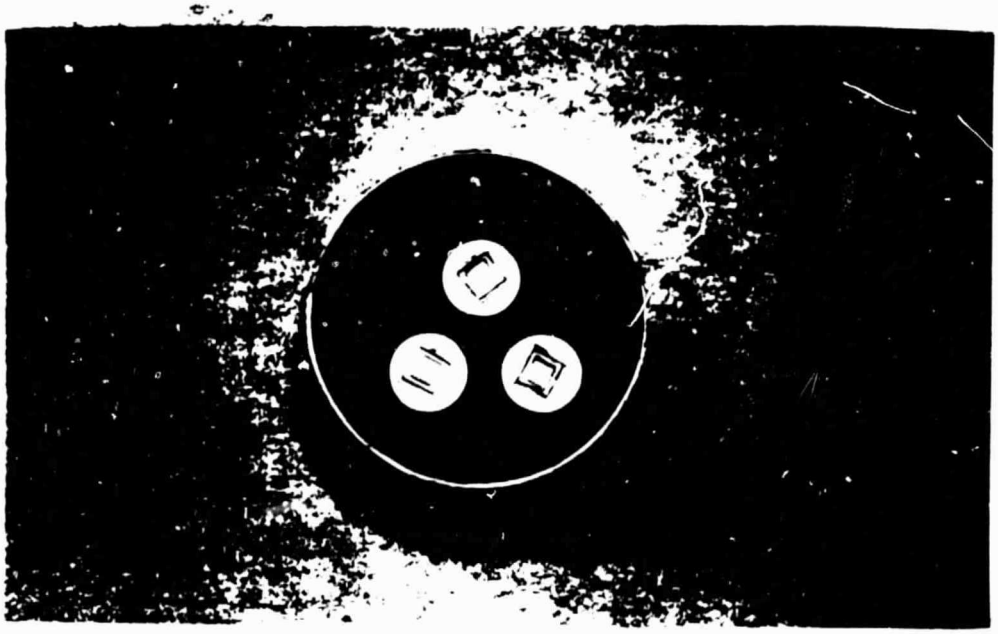

Figure 31: Polished disks and three more assemblies placed on first set.

Figure 32: Finished HIP container with lid welded on.

canning procedure are summarized in table 4.

The HIP welding procedure consisted of the following:

1) The sealed can was positioned on the HIP's resistive heating assembly with ceramic spacers as shown in figure 33.
2) The thermal barrier package was slipped over the can and fastened down as shown in figure 34.
3) The entire thermal barrier assembly was placed in the HIP's pressure vessel, which was then sealed.
4) A typical weld cycle is as shown in figure 35. The temperature was raised to 250 C in 15 minutes. The pressure was then raised as quickly as possible to the weld level, as the temperature was simultaneously raised further. The heating rate was controlled so that the temperature and pressure would reach their weld levels at approximately the same time. After holding at the weld levels for the appropriate period of time, the temperature was ramped down. Once the temperature reached the ambient, the pressure was released quickly. The welding parameters used in each HIP run

are included in table 4.

Table 4: Hot Isostatic Welding Procedures

| Run # | Temp. | Pressure | Hold Time | Cool Time | Pressure Medium | Container Type |
|---|---|---|---|---|---|---|
| 1 | 350 | 15 | 30 | 30 | graphite | 1.5 in. long 0.75 in. dia. steel and Al |
| 2 | 350 | 15 | 30 | 30 | graphite and quartz | 0.75 in. dia. can inside 3 in. long 3 in. dia. steel can |
| 3 | 350 | 10 | 15 | 30 | graphite | 4.5 in. long 3 in. dia. steel |
| 4 | 350 | 2.5 | 60 | 30 | graphite | 3 in. long 3 in. dia. steel |
| 5 | 350 | 2.5 | 30 | 60 | graphite | 3 in. long 3in. dia. steel |
| 6 | 450 | 2.5 | 30 | 90 | graphite | 2 in. long 3 in. dia. steel |
| 7 | 450 | 2.5 | 30 | 90 | graphite | 2 in. long 3 in. dia. steel |
| 8 | 250 | 5 | 30 | 90 | graphite | 2 in. long 3 in. dia. steel |
| 9 | 250 | 2.5 | 30 | 45 | graphite | 2 in. long 3 in. dia. steel |
| 10 | 350 | 1.25 | 30 | 60 | graphite | 2 in. long 3 in. dia. steel |

Table 4: Continued

| Run # | Temp. | Pressure | Hold Time | Cool Time | Pressure Medium | Container Type |
|---|---|---|---|---|---|---|
| 11 | 350 | 2.5 | 30 | 120 | graphite | 2 in. long 3 in. dia. s |
| 12 | 450 | 1.25 | 30 | 150 | graphite | 2 in. long 3 in. dia. s |
| 13 | 300 | 3.7 | 30 | 60 | graphite | 2 in. long 3 in. dia. s |
| 14 | 250 | 3.7 | 30 | 60 | graphite | 2 in. long 3 in. dia. s |

Note: Temperatures in C

Pressure in ksi

Time in minutes

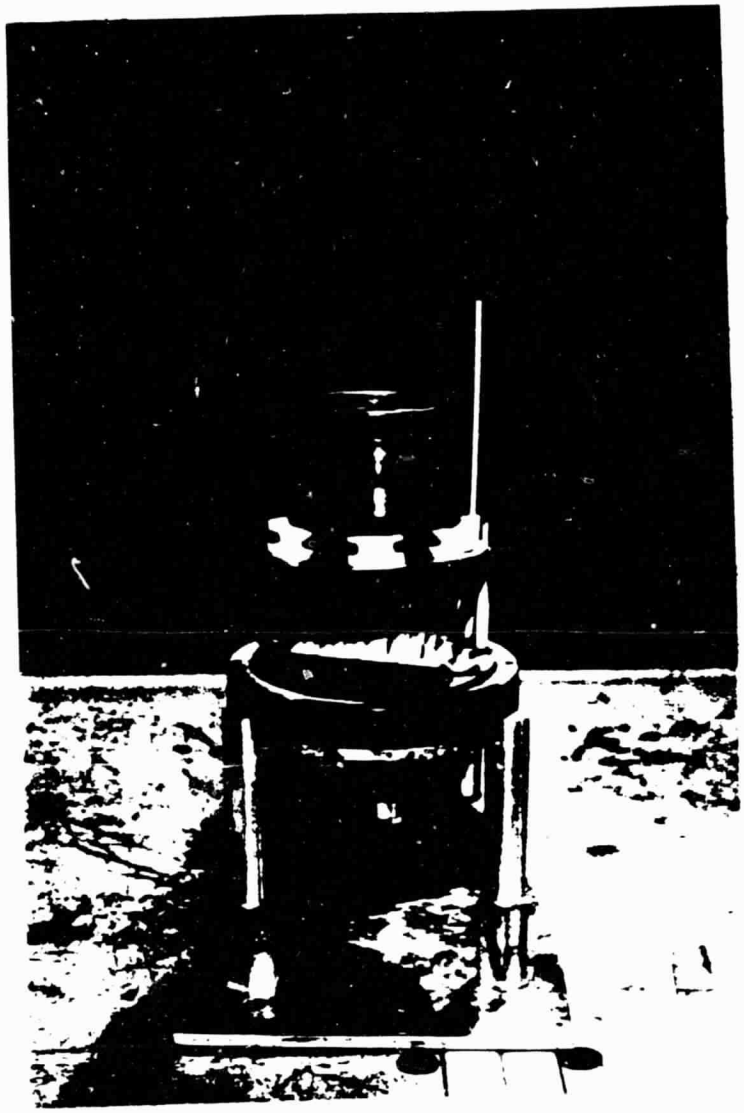

Figure 33: HIP container positioned on resistive heating assembly.

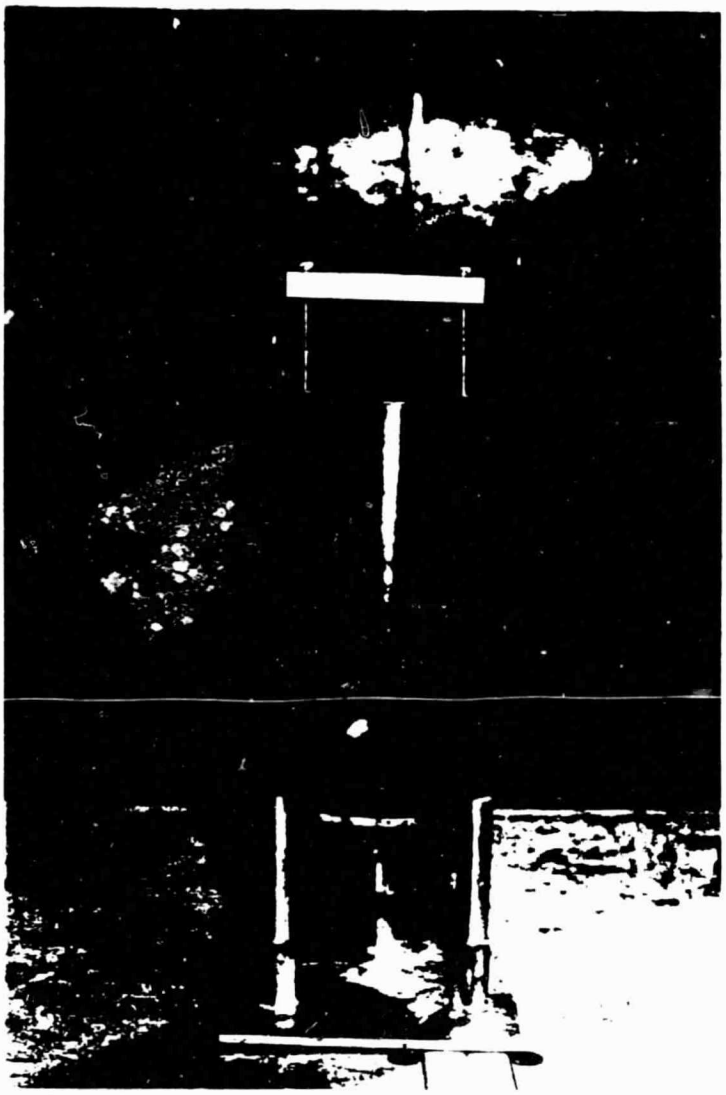

Figure 34: Thermal barrier package fastened in place.

**Testing**

The steel coupons welded with the Gleeble were tested with an Instron tensile testing machine, using a crosshead speed of 0.02 in./min. The parts were clamped in serrated jaws such that the joints failed in shear. Accuracy of the tests was estimated to be within 30 lb.

The HIP welded mockups of the cell stack assembly were peel tested to reveal the degree of bonding. The peel tests were conducted under distilled water to prevent the spread of BeO particles. The fracture surfaces were then inspected at various magnifications with a scanning electron microscope (SEM).

An attempt was made to conduct quantitative mechanical tests on the HIP welded assemblies with the testing device shown in figure 36. The assemblies were clamped between two mandrels, such as the one shown in figure 37. One mandrel was fixed, and the other was free to spin in a linear bearing. Weights were hung from lever arms attached to the free mandrel, and the joints were thus stressed in torsion. The device only worked for poorly bonded samples because the parts tended to slip from the mandrels. A redesigned clamp for the parts might make the torsion tester usable for future work.

In addition to the peel tests and SEM

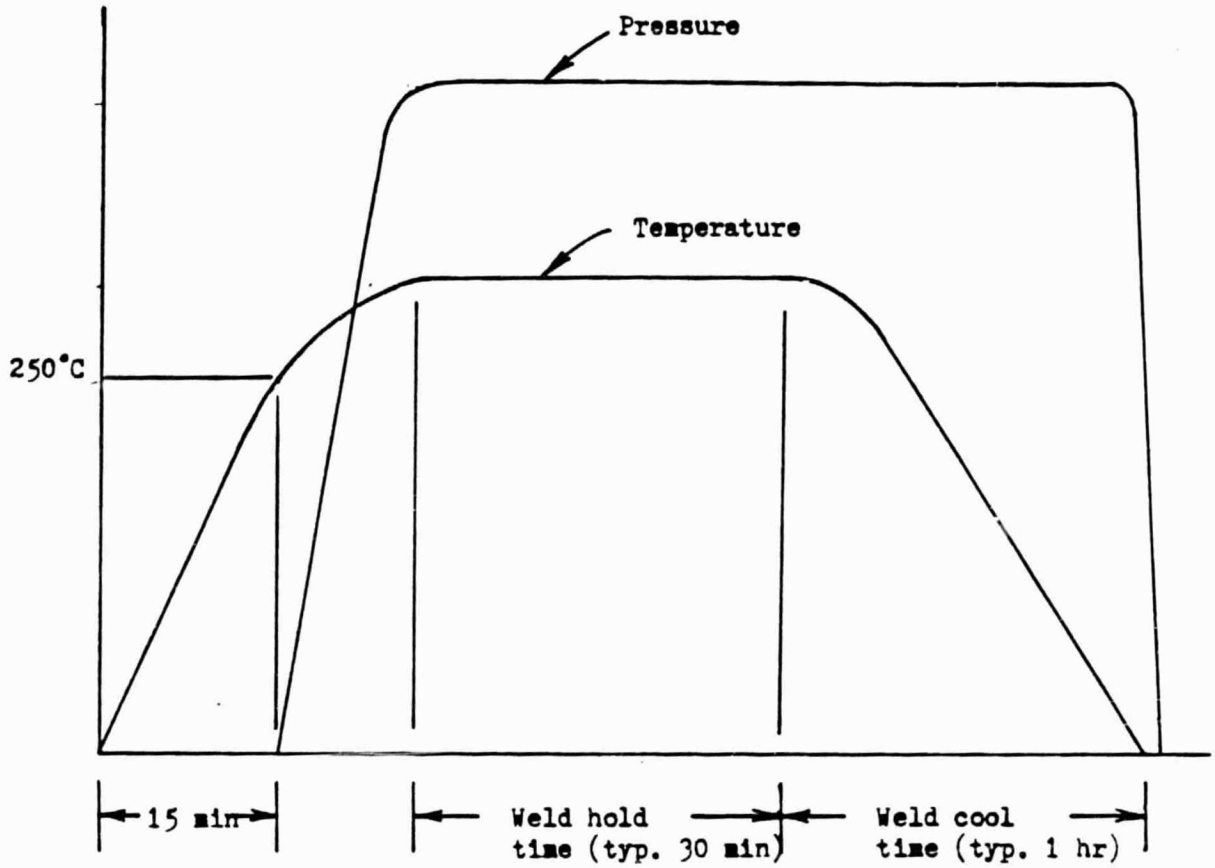


Figure 35: Typical HIP weld cycle

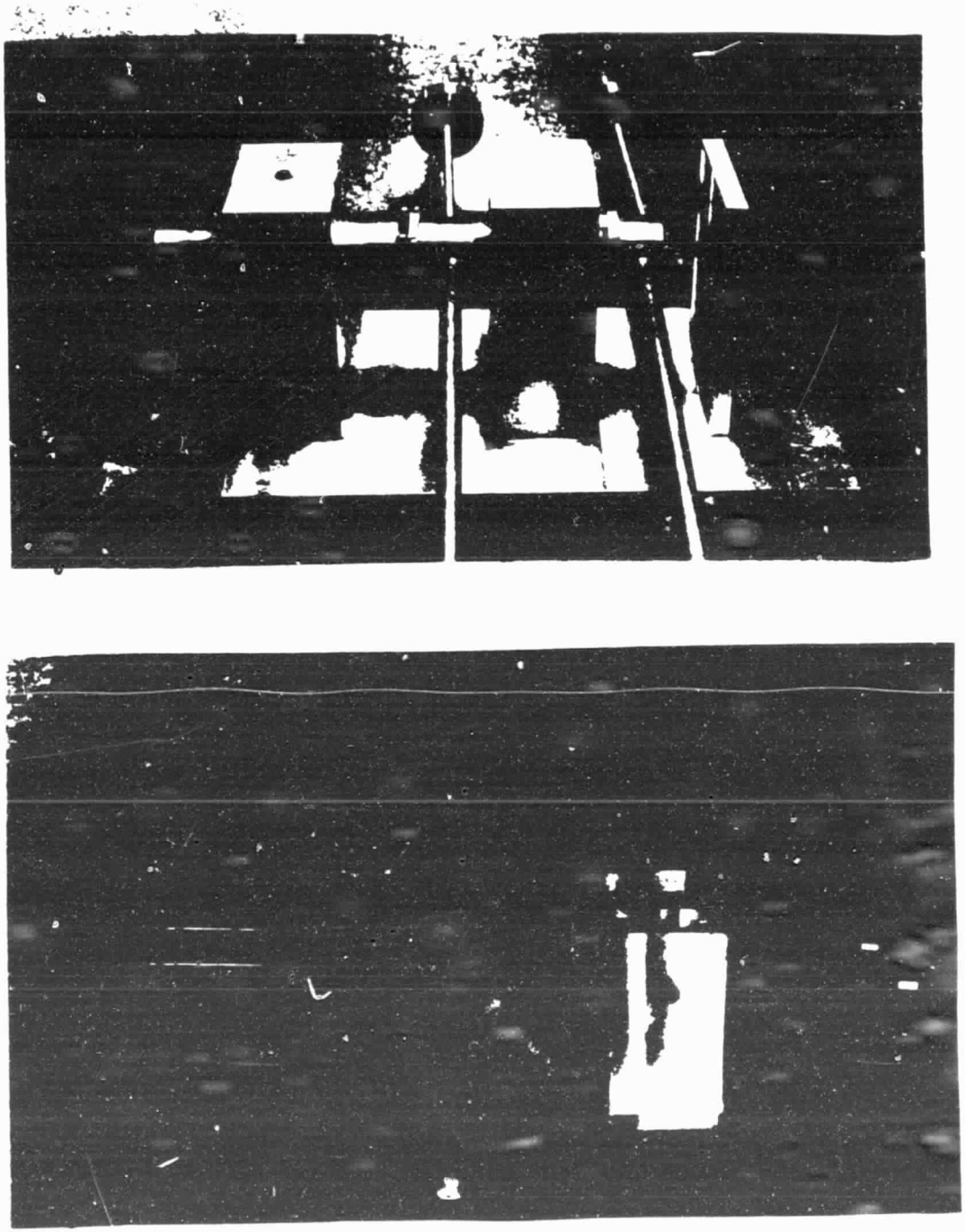

Figure 36: Torsion testing device for HIP welded assemblies.

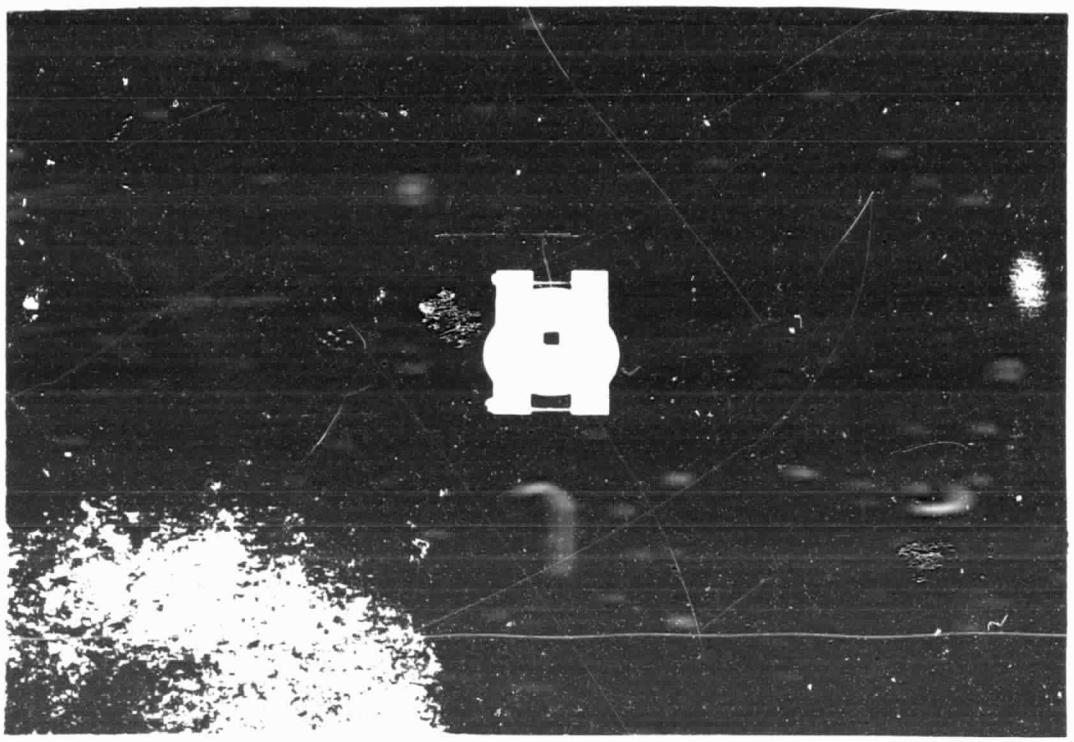

Figure 37: Mandrel for torsion tester.

observations, the HIP welded assemblies were evaluated by visual inspection under low magnification (up to 70X). The inspection primarily concerned the severity of cracking in the GaAs.

## RESULTS AND DISCUSSION

### Gleeble Study

The results of the welds made on silver plated steel coupons are presented in figures 38 through 46. Figure 38 contains the entire data set, plotted with weld strength as a function of welding pressure, for several temperatures. The same data is shown again as individual curves in figures 39 through 45, for clarity. In figure 46, the data is plotted again, with weld strength as a function of welding temperature, at 10,000 psi welding pressure. The gleeble's unpredictable servo control did not allow the exact same pressures to be used at the different temperatures. Therefore, the data plotted in figure 46 were generated by averaging the results near 10,000 psi when necessary.

The results plotted in figure 38 form two relatively distinct bands at high pressures, and appear to merge at pressures below 10,000 psi. The upper band includes the results of welds made at temperatures of 300 C or higher, whereas the results in the lower band are for temperatures of 250 and 275 C. Much of the separation between curves may be ascribed to experimental error. The two distinct bands might,

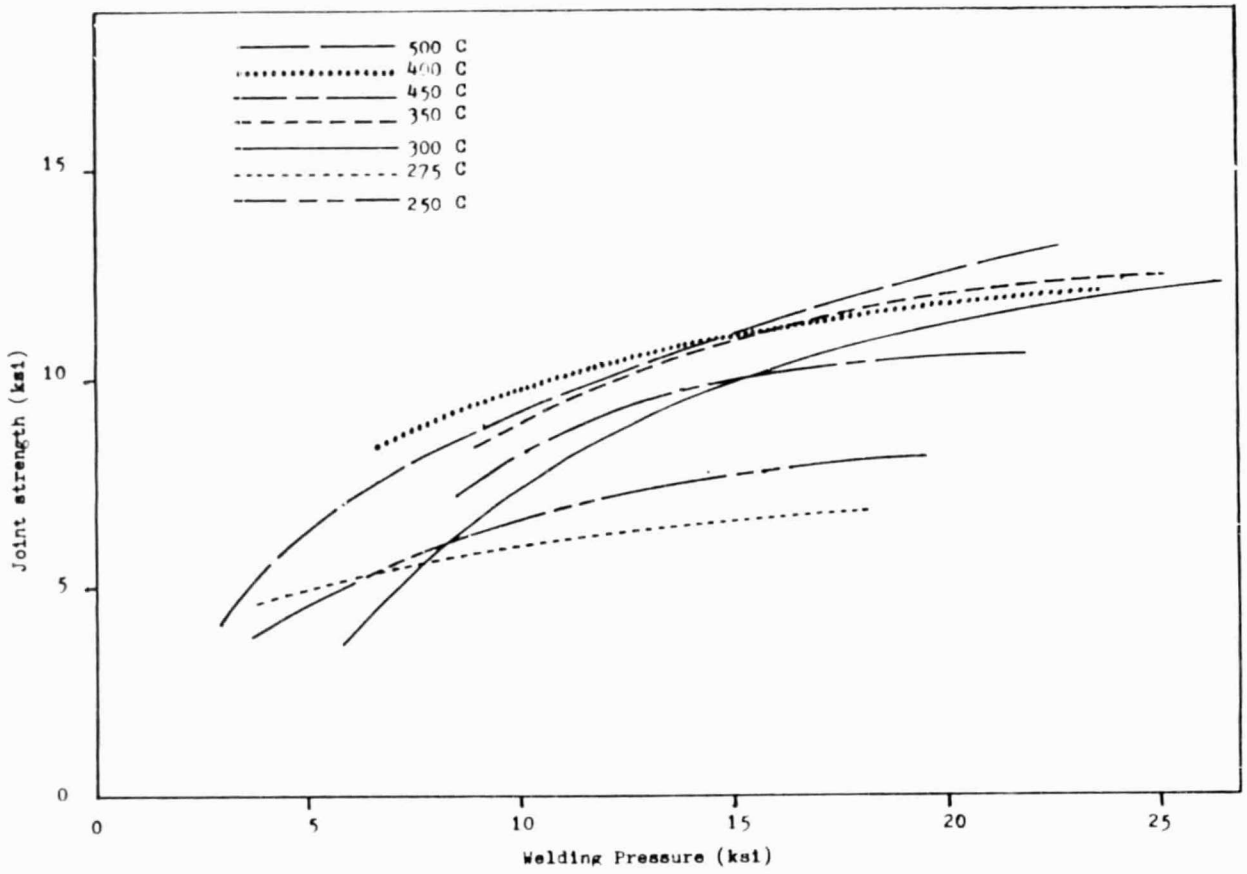


Figure 38: Joint strength vs. welding pressure for all temperatures considered

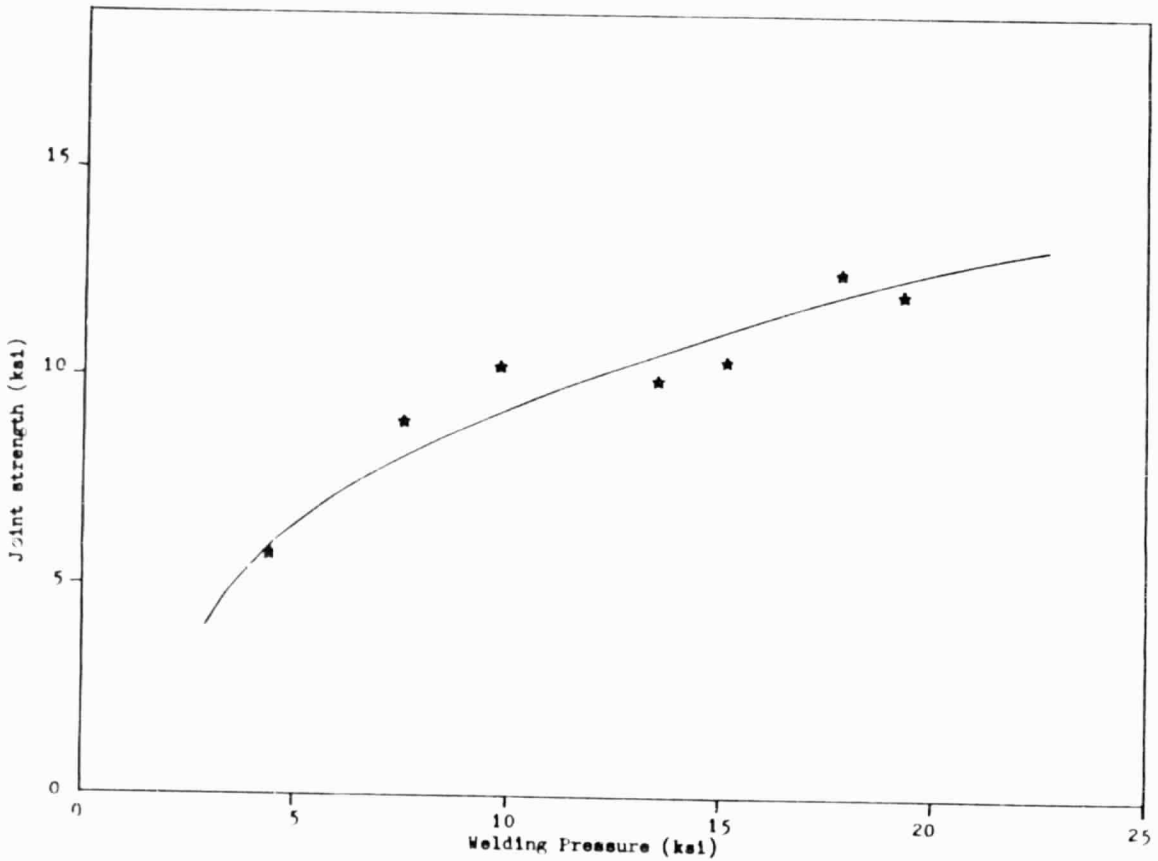


Figure 39: Joint strength vs. welding pressure for a welding temperature of 500°C

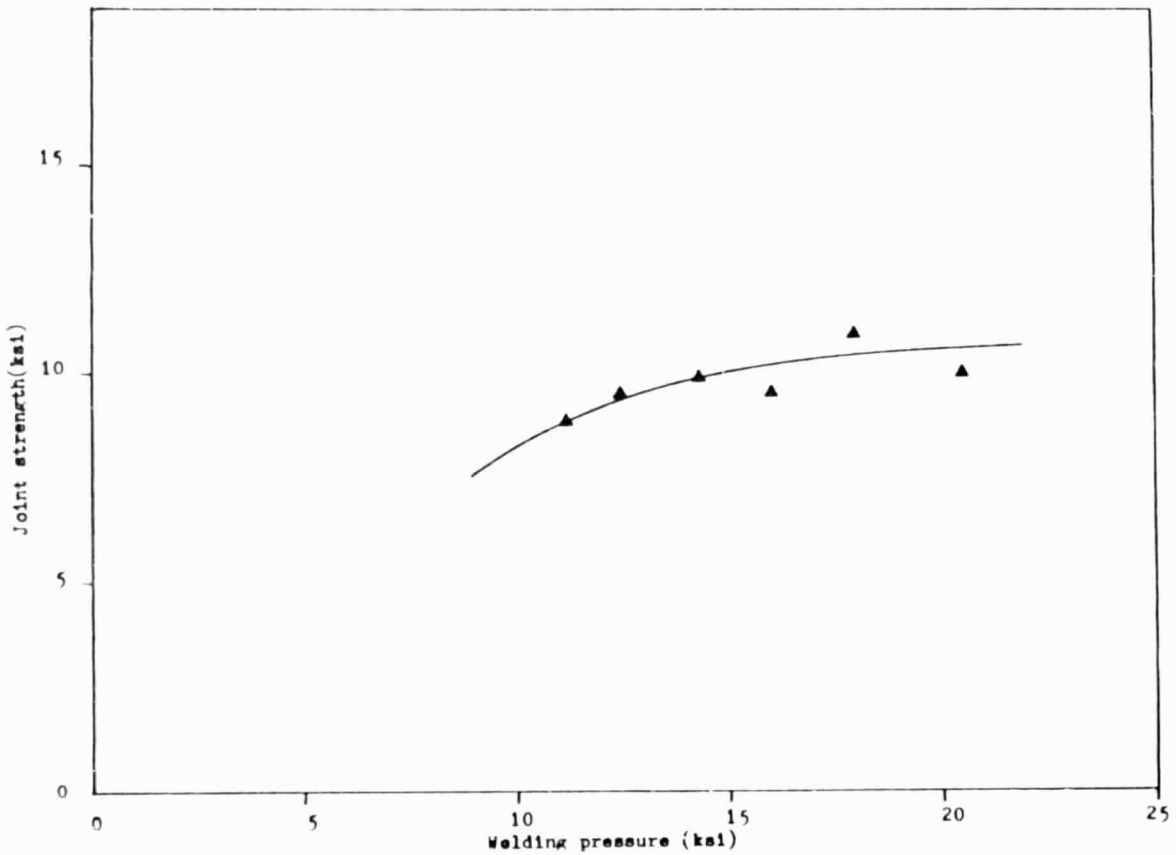


Figure 40: Joint strength vs. welding pressure for a welding temperature of 450°C.

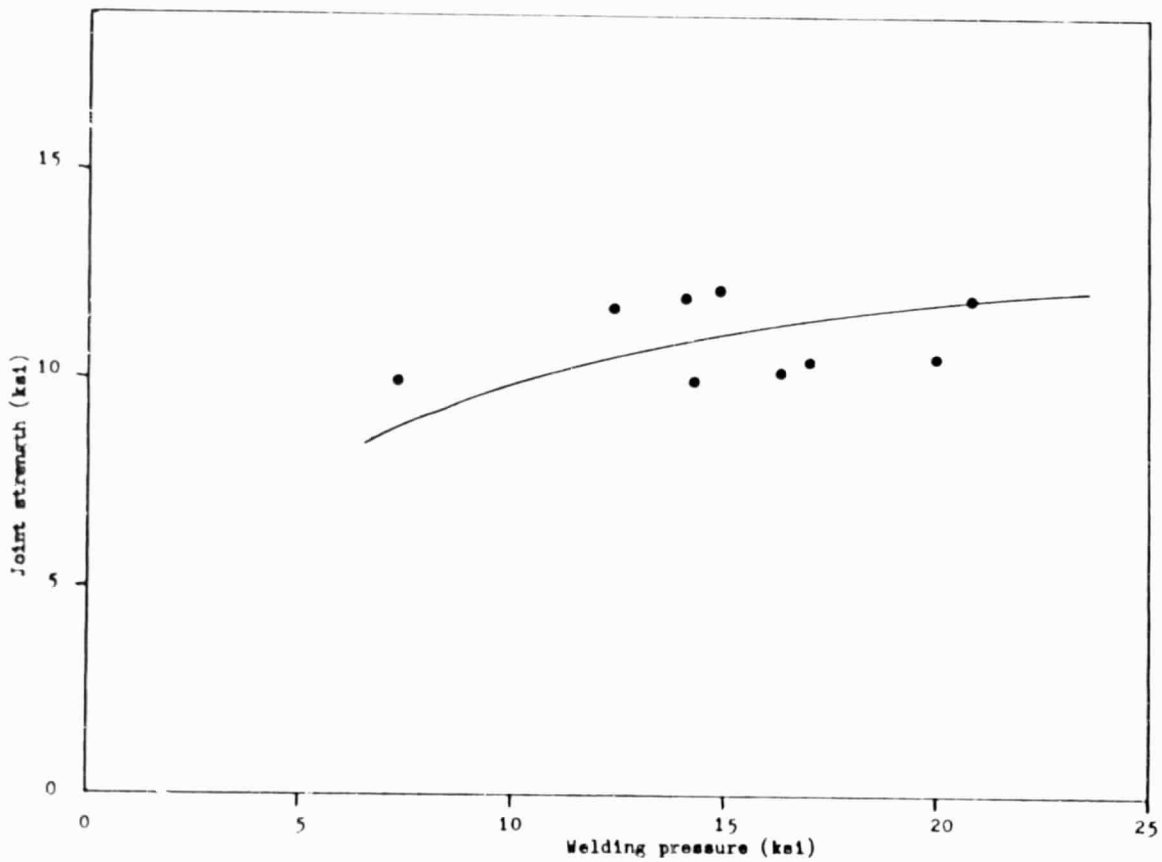


Figure 41: Joint strength vs. welding pressure for a welding temperature of 400°C.

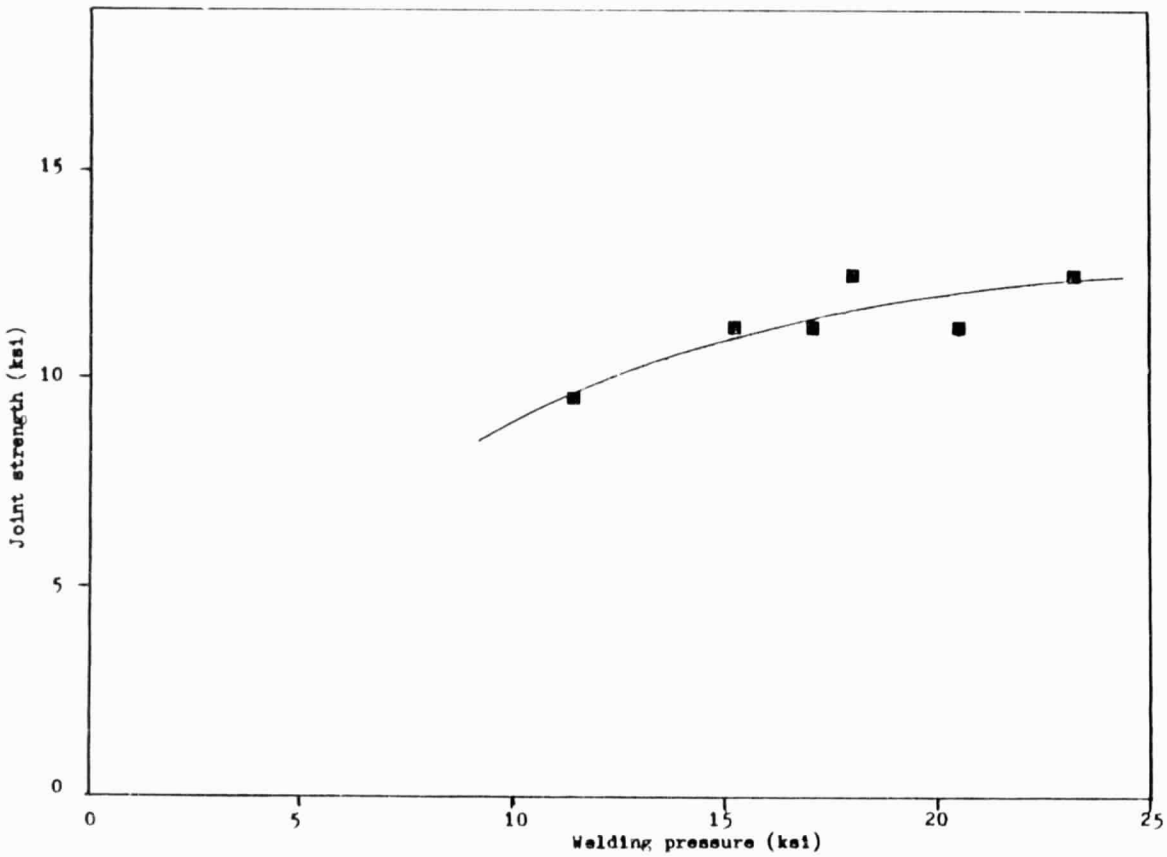


Figure 42: Joint strength vs. welding pressure for a welding temperature of 350°C.

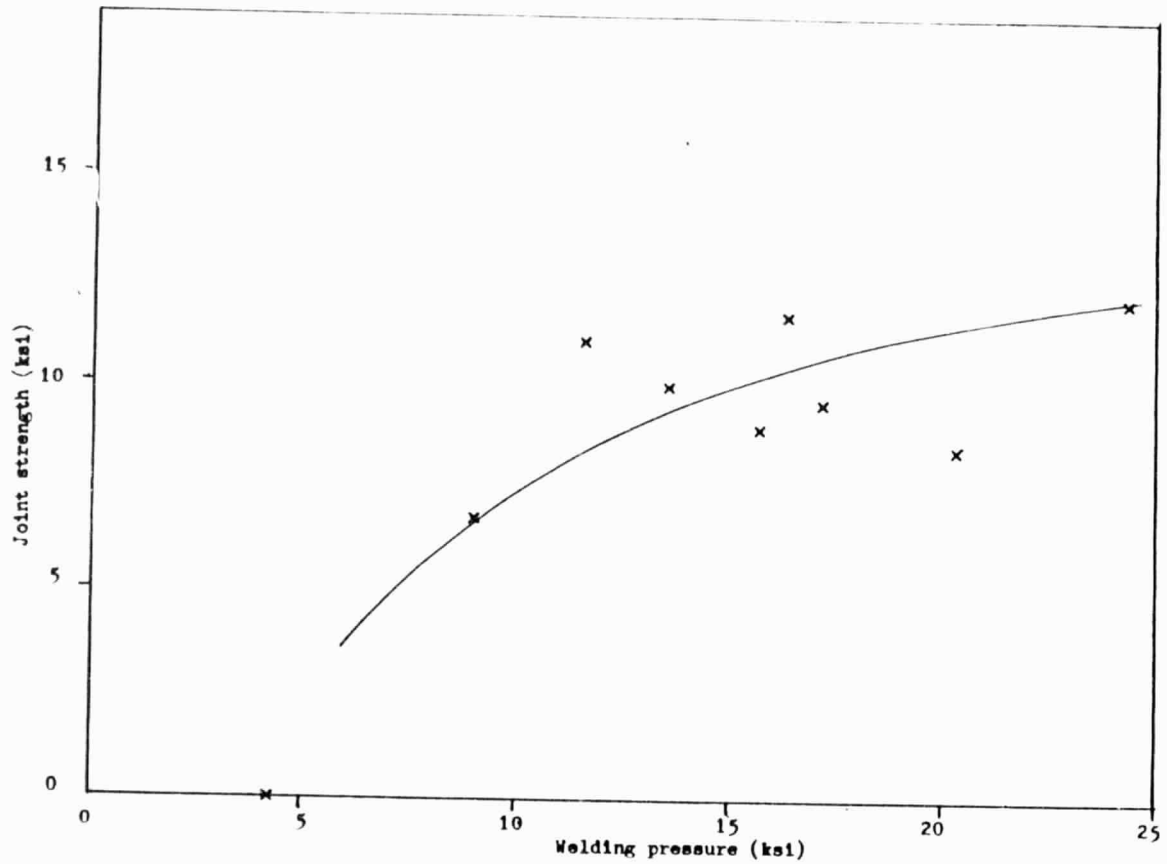


Figure 43: Joint strength vs. welding pressure for a welding temperature of 300°C.

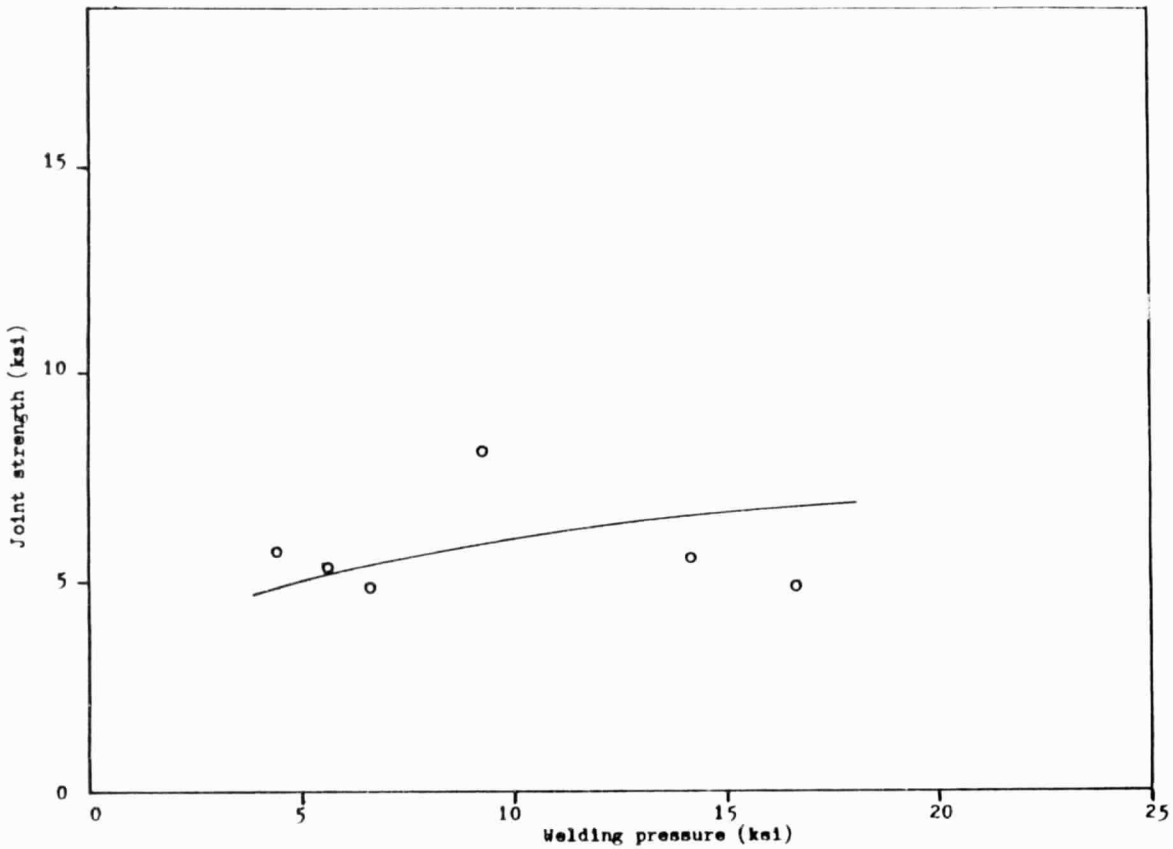


Figure 44: Joint strength vs. welding pressure for a welding temperature of 275°C.

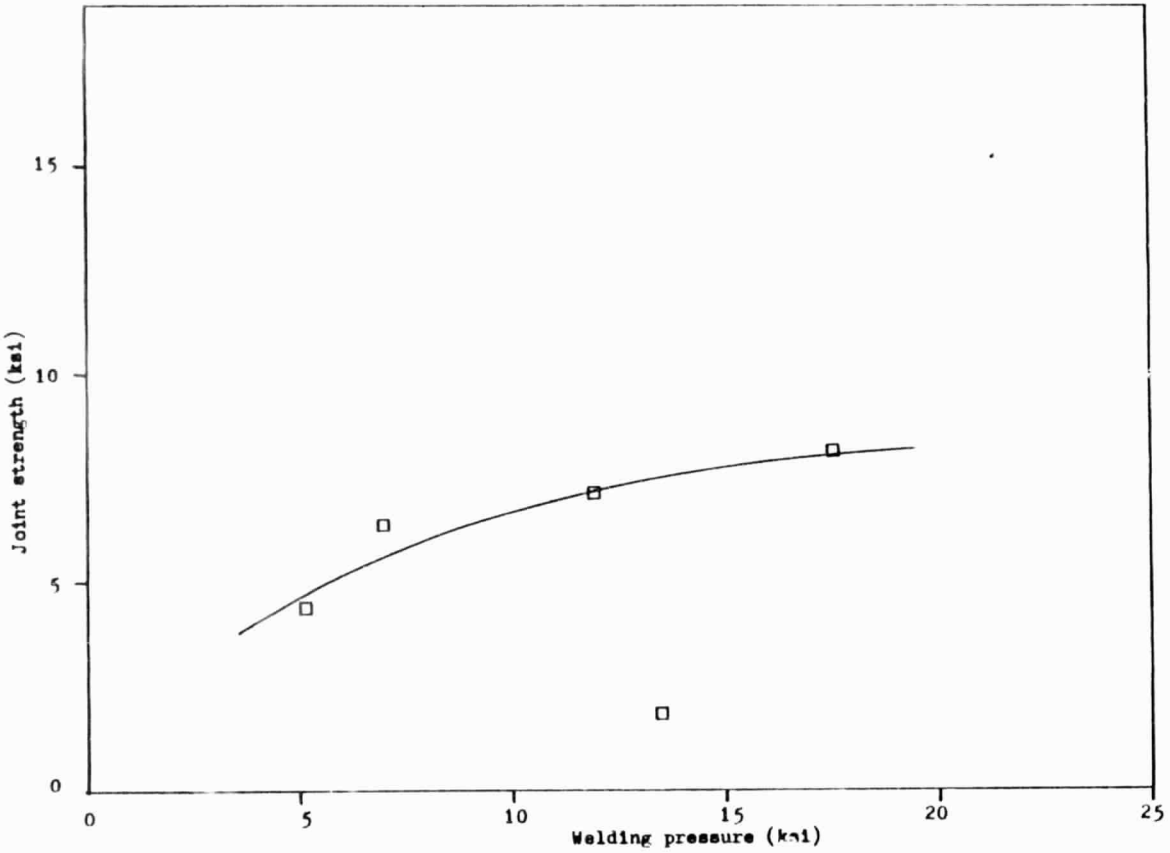


Figure 45. Joint strength vs. welding pressure for a welding temperature of 250°C.

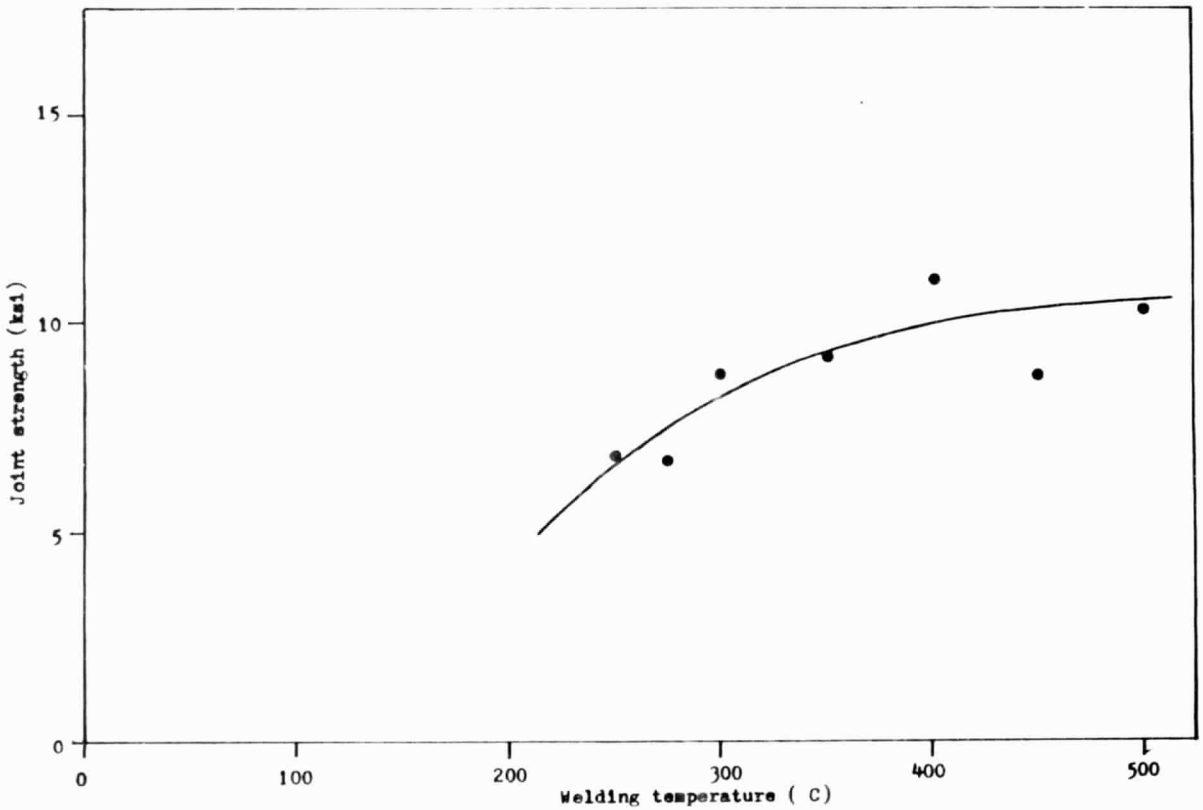


Figure 46: Joint strength vs. welding temperature for a welding pressure of 10,000 psi.

however, have resulted from the effects of one of the mechanisms for welding described in the background. A likely candidate would be recrystallization, as the greater microscopic plastic deformation occurring at higher pressures might magnify the effects of temperature. In any event, one may safely state that, at pressures above 10,000 psi and temperatures above 300 C, further increases in temperature will provide little improvement in strength. This is illustrated in the curve of figure 46, which levels out at about 300 C.

Also of interest are the results of welds made at 225 and 200 C. All but two of the welds made at 225 C fell apart during handling. The two assemblies which survived exhibited relatively low strengths, even though they were welded at high pressure. None of the assemblies processed at 200 C survived handling.

The effect of pressure increases also appeared to decrease at high levels. The average increase in strength was 3000 psi when the pressure was raised from 5000 to 10000 psi, while a further increase to 15000 psi pressure typically improved the strength by only 1600 psi.

## HIP Study

**Encapsulation**. As was described in chapter 4, the encapsulation procedure for the HIP welded assemblies underwent an evolution over the course of the first 6 runs. The difficulty lay in achieving true isostatic stress on the assemblies. Although pressure from the argon gas was always isostatic on the outside surface of the container, non-uniform collapse of the container altered the state of stress, since the granular transfer medium was not truly fluid. A liquid pressure transfer medium would have provided isostatic stress to the assemblies regardless of the container collapse, but no means were available to prevent penetration of a liquid into the joints.

In the worst cases, the non-uniform stress resulted in severe distortion of the assemblies, as in runs 2 and 3. The container design was never developed to the point where the stress could be considered truly isostatic, but the final design did provide a consistent, symmetricl collapse. Only a spherical container or one made of a very flexible material such as an elastomer could be expected to collapse uniformly.

The original procedure called for small cans with an inside diameter only slightly larger than the

diagonal of the Cu component. The rationale was to minimize the volume of granular material required, and thus the amount the container must collapse to transfer the pressure. This design failed primarily because the containers could not be reliably sealed with the available equipment. It was also discovered in later runs that a certain minimum layer of granular material was required between the assemblies and the container, to prevent damage. The minimum spacing was estimated to be 0.5 in. before collapse, which would not have been provided by the small containers.

The 3" diameter steel containers collapsed as shown in figure 47. The dished lids bent with a maximum deflection at the center, as defined by the following equation:(66)

$$\Delta_{max} = 0.1705\ P\ r^4 / (E\ t^3)$$

where $\Delta_{max}$ = maximum deflection

P = pressure

r = radius of lid

t = thickness of lid

and E = modulus of elasticity

Since the dimensions of the lids were fixed, their deflection depended only on the pressure used.

The collapse of the cylindrical section of the

Figure 47: Collapsed HIP container.

containers occurred by buckling with several nodes. The deflection was therefore difficult to predict, since it depended on the effective restraint imposed by the dished lids and the material inside the can. The effective restraint increased significantly as the length of the can decreased, and as the density of the granular pressure medium increased.

The length of the can had the most significant influence on the effective restraint. When the cylindrical section was 3 in. long, the collapse occurred with 7 nodes, and was not symmetric about the longitudinal axis. When the length was decreased to 2 in., the number of buckling nodes increased to 9, and the collapse was much more symmetrical.

Of the three pressure transfer media used - fused quartz crystal, graphite and alumina - graphite was by far the most acceptable. The other two materials tended to clot together during the welding cycle, and thus did not flow properly. The clotting also hampered removal of assemblies from the containers, increasing the risk of damage during handling. The mesh size of the pressure medium proved to be of some importance also, as it affected both the collapse of the container and the ability to form around the assemblies. A very fine

powder tends to be denser than larger granules, and thus does not require as great a collapse of the container. Finer particles also tend to conform around the assemblies better, and provide more even pressure application. For these reasons, the granular graphite was crushed into a fine powder for the later runs, using a mortar and pestle.

**Strength**. The results of the HIP welding tests are summarized in table 5. Quantitative mechanical testing was unsuccessful, so relative strengths were determined from examination of the fracture surfaces of peel tested BeO-Cu joints. The percent bonded areas given in table 5 were estimated from low magnification SEM photographs, and represent the areas where bonding was great enough to tear the silver coating from the substrate. These areas were simply the easiest to detect, and were not necessarily the only areas of bonding.

The SEM macrographs are displayed in figures 49 through 52. In most cases, the silver coating was torn from the substrate in a ring near the outer diameter. This region of sound welding was probably caused by a slight upset of the copper component. A typical sample is shown in cross section in figure 53. In the band of sound welding the copper was compressively deformed.

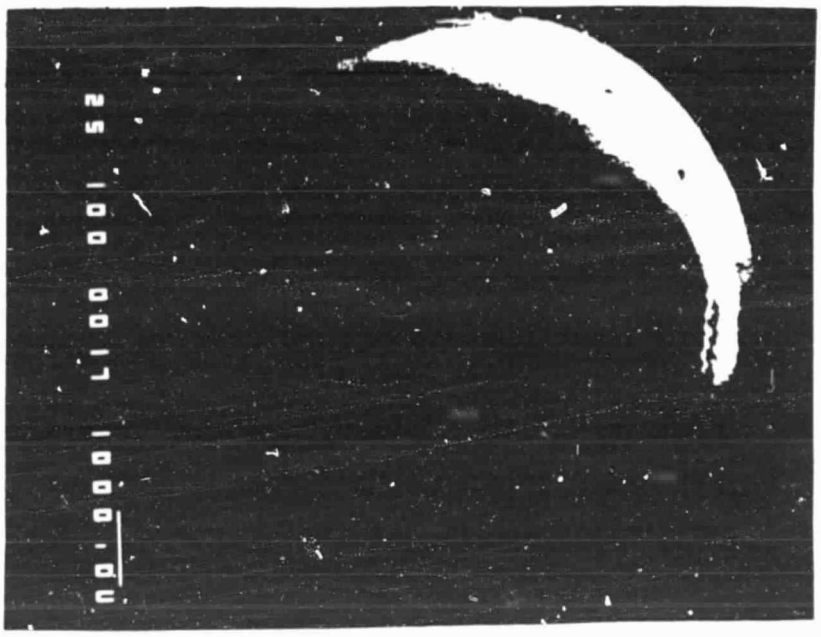


a) Welding pressure 5000 psi

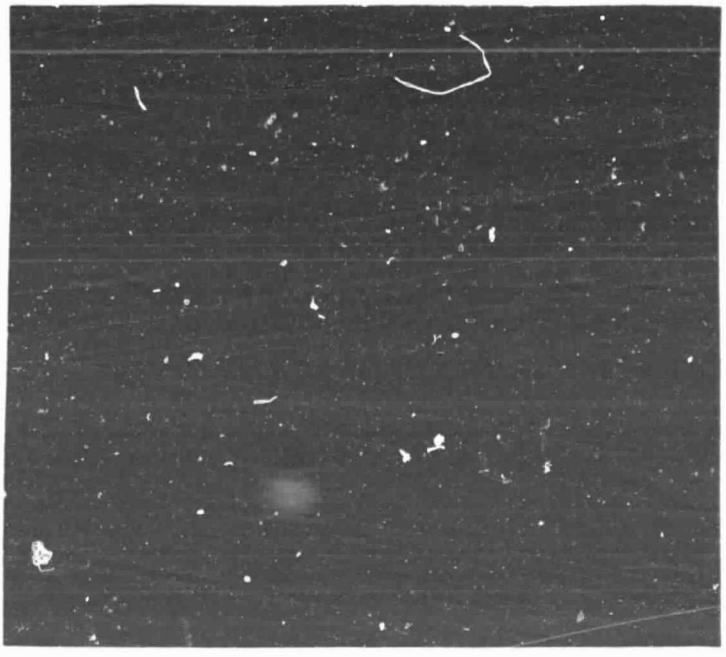

b) Welding pressure 2500 psi

Figure 48: Fracture surfaces of joints welded at 250 C.

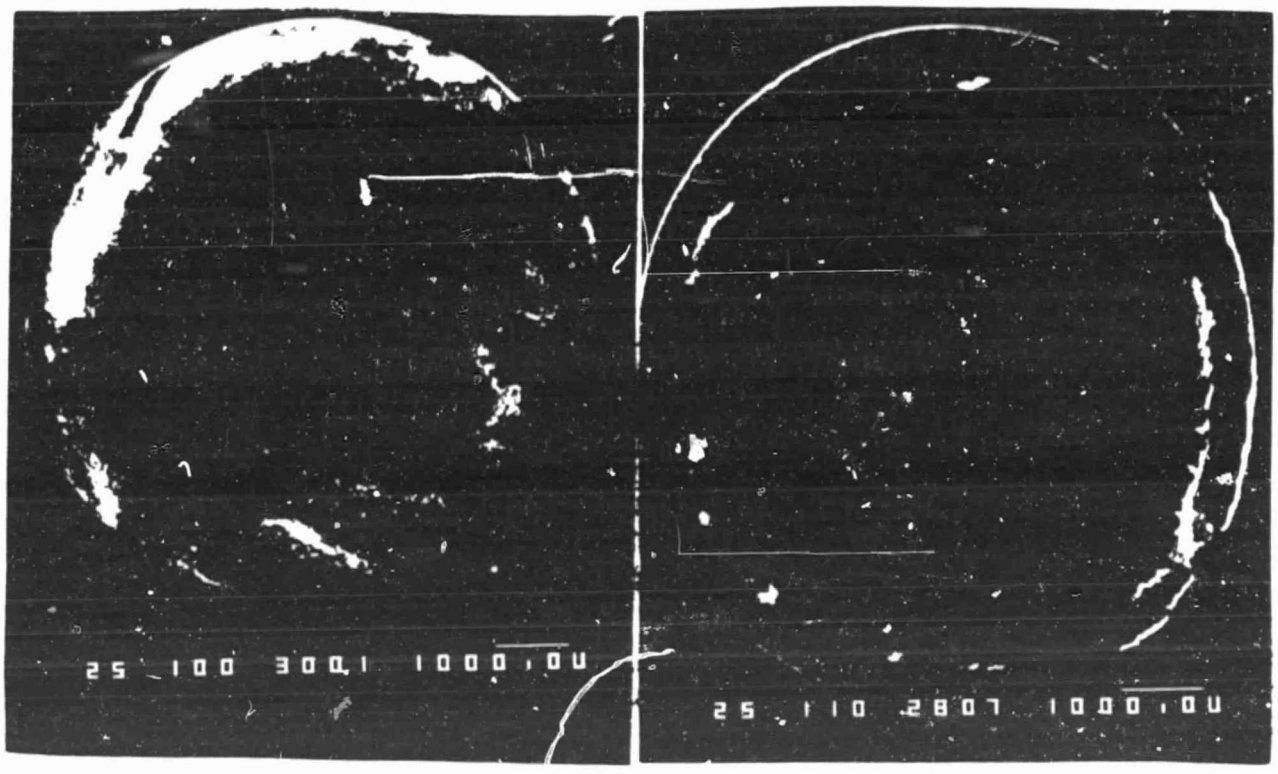


a) Welding pressure 10,000 psi

b) Welding pressure 2500 psi

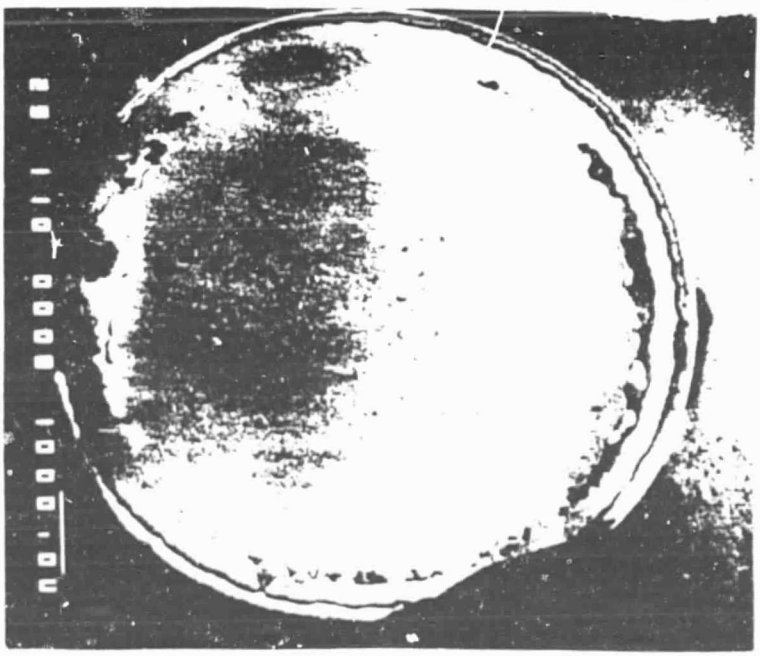

c) Welding pressure 1250 psi

Figure 49: Fracture surfaces of joints welded at 350 C.

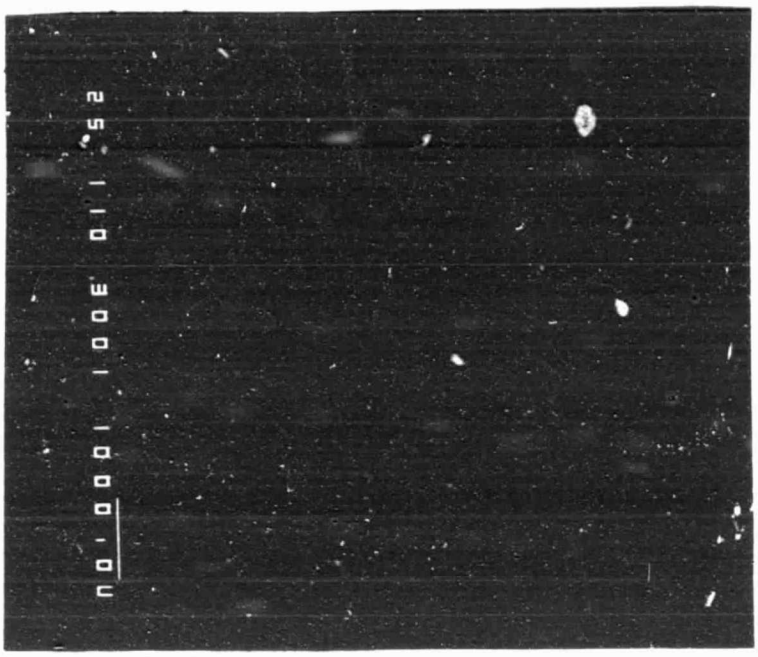

a) Welding pressure 2500 psi

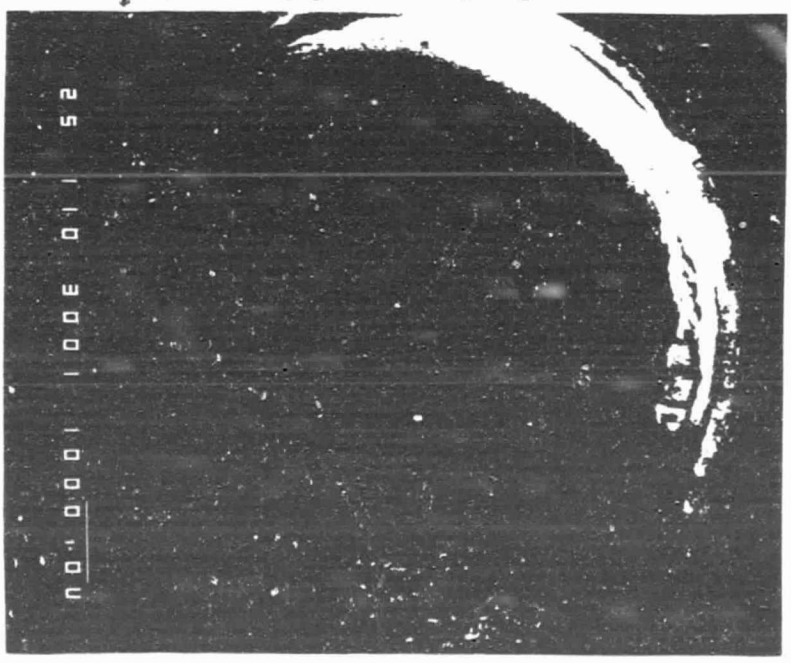

b) Welding pressure 1250 psi.

Figure 50: Fracture surfaces of joints welded at 450 C.

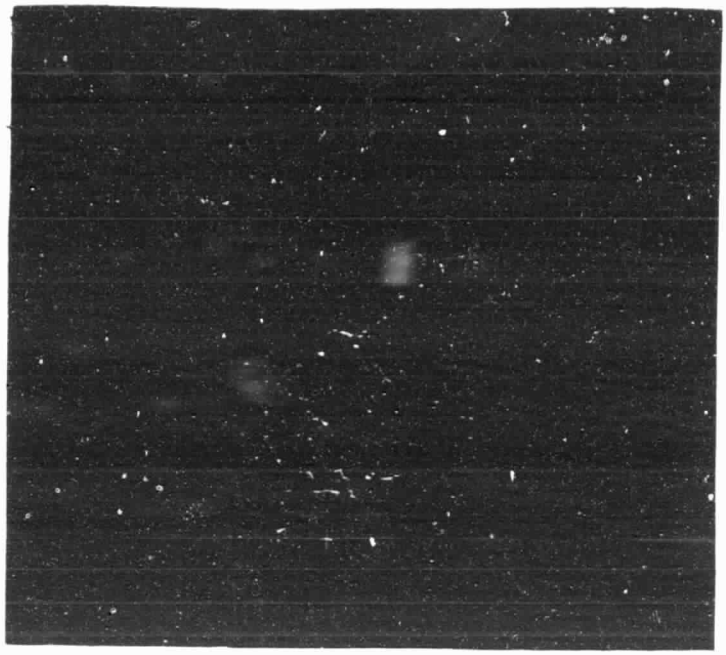

a) Copper side

b) Beryllia side

Figure 51: Fracture surfaces of joint welded at 300 C and 3700 psi.

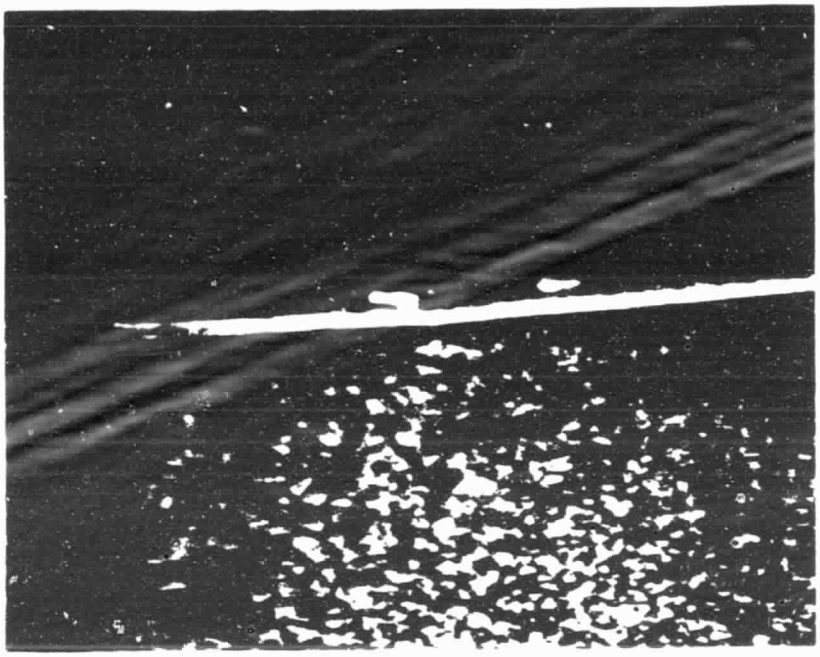

Figure 52: Cross section of typical HIP welded joint.

Table 5: Summary of HIP welding results

| Run # | Temp. | Pres. | Hold Time | Cool Time | Part Condition | % Area Bonded | Comments |
|---|---|---|---|---|---|---|---|
| 1 | 350 | 15 | 30 | 30 | ---- | ---- | Container leaked |
| 2 | 350 | 15 | 30 | 30 | severely distorted | ---- | |
| 3 | 350 | 10 | 15 | 30 | severely distorted | ---- | |
| 4 | 350 | 2.5 | 60 | 30 | 1 assembly only undamaged | ---- | |
| 5 | 350 | 2.5 | 30 | 60 | 3 assy.'s undamaged | 20 | |
| 6 | 450 | 2.5 | 30 | 90 | all assy's damaged | ---- | poor can design |
| 7 | 450 | 2.5 | 30 | 90 | all assy's damaged | 50 | |
| 8 | 250 | 5 | 30 | 90 | 1 assembly only undamaged | 5 | |
| 9 | 250 | 2.5 | 30 | 45 | all assy's undamaged | 0 | |
| 10 | 350 | 1.25 | 30 | 60 | all assy's undamaged | 10 | |

| | | | | | | | |
|---|---|---|---|---|---|---|---|
| 11 | 350 | 2.5 | 30 | 120 | all assy's slightly cracked | 20 | |
| 12 | 450 | 1.25 | 30 | 150 | 1 without damage others cracked | 10 | |
| 13 | 300 | 3.7 | 30 | 60 | all assy's cracked | 25 | |
| 14 | 250 | 3.7 | 30 | 60 | All assy's undamaged | 0 | |

Note: Temperature in C

Pressure in ksi

Time in minutes

Exterior to this band the copper was lifted away from the BeO. This condition resulted from the large difference in plasticity between the two materials, and the lack of true isostatic stress.

In the samples welded at low temperatures and pressures, the areas where the coating was separated from the substrate occurred in a regular pattern across the surface. The pattern corresponded to visible surface features on the BeO components, left by the surface grinding technique. Photographs of each side of a fractured joint surface are displayed in figure 52. The surface features correspond to areas of failure either at the coating - substrate interface, or within the substrate itself. The fact that the topography on the copper side was generally elevated, while that on the BeO side was depressed, indicates that failure occurred in the BeO component.

The best strength occurred in the sample welded at 350 C and 10,000 psi. The failure surface, shown at high magnification in figure 53, was entirely within the BeO. This indicates that the coating methods of this study would have adequate adherence if BeO were used as the pad material. The next best strength resulted from welding at 450 C and 2500 psi. The Cu side of the

Figure 53: Fracture surface of joint welded at 350 C and 10000 psi. 3000X

fracture surface is shown at higher magnifications in figure 54. The silver coating was clearly torn away from the Cu in many areas. The coating itself displayed a dimpled surface, characteristic of ductile failure. Failure probably occurred within the silver layer at these locations.

The fracture surface of the joint welded at 350 C and 2500 psi is shown at several magnifications in figures 55 and 56. At 200X, it is clear that the coating was torn from the BeO at many locations. In between, however, there are several much smaller areas where the silver was apparently torn from the Cu and remained adhered to the BeO. Figure 55b is a 2400X shot of the edge of one of the "craters" formed when the coating was torn away. Figure 56a is a photograph of the silver coating a small distance from the crater. The "spongy" or dimpled areas are locations where failure occurred within the silver layer. In the surrounding areas bonding was apparently minimal, either because of lack of contact, or contamination. The surface of the "crater" is shown at 3900X in figure 56b. This appears significantly different than the BeO fracture surface shown in figure 54. The different surface features in figure 56b may have resulted from the fact that the

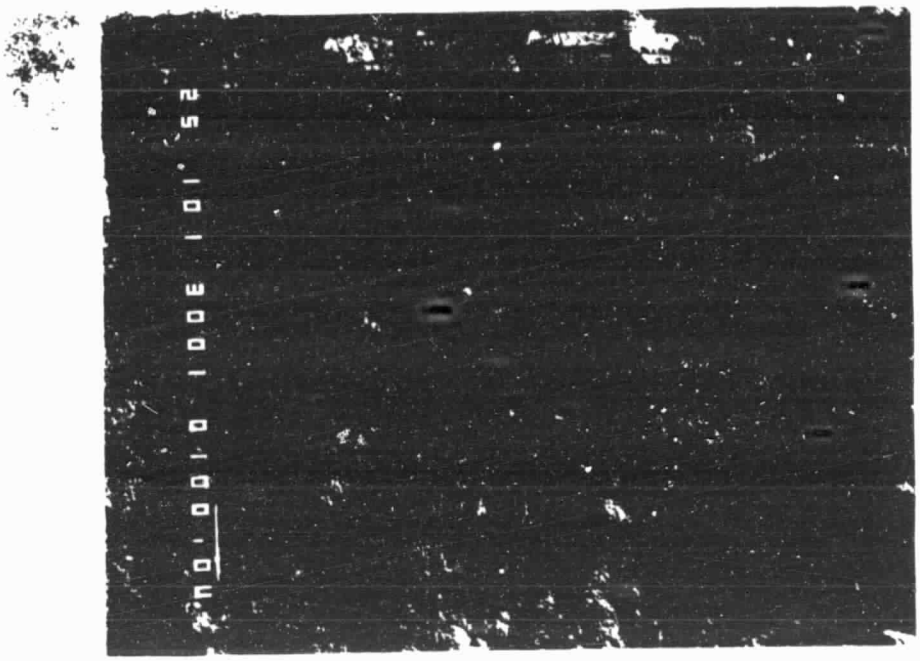

a) 100X

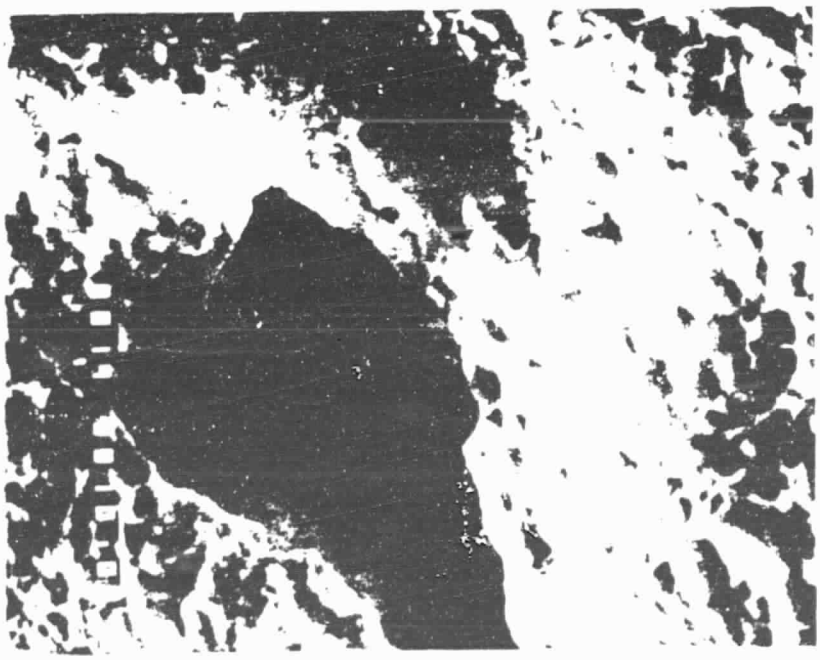

b) 1000X

Figure 54: Fracture surface of joint welded at 450 C, 2500 psi.

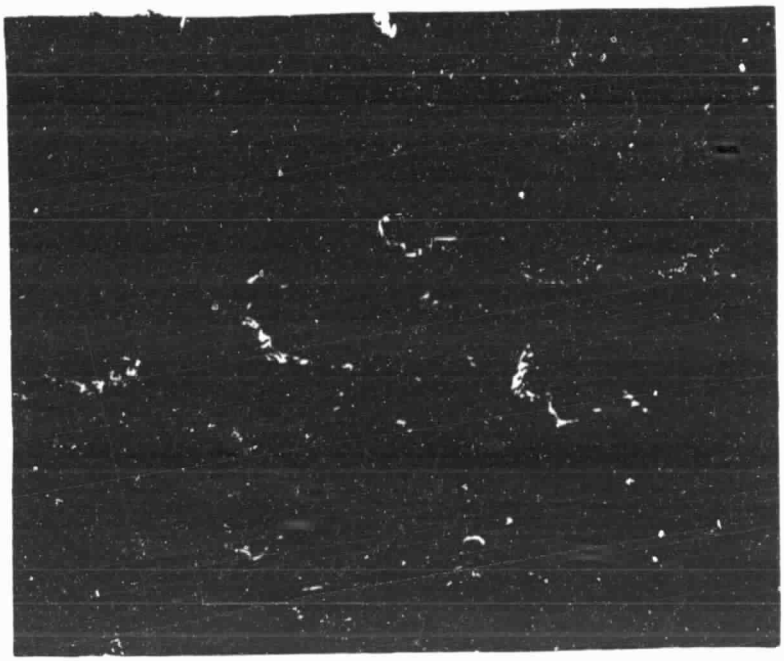

a) 200X

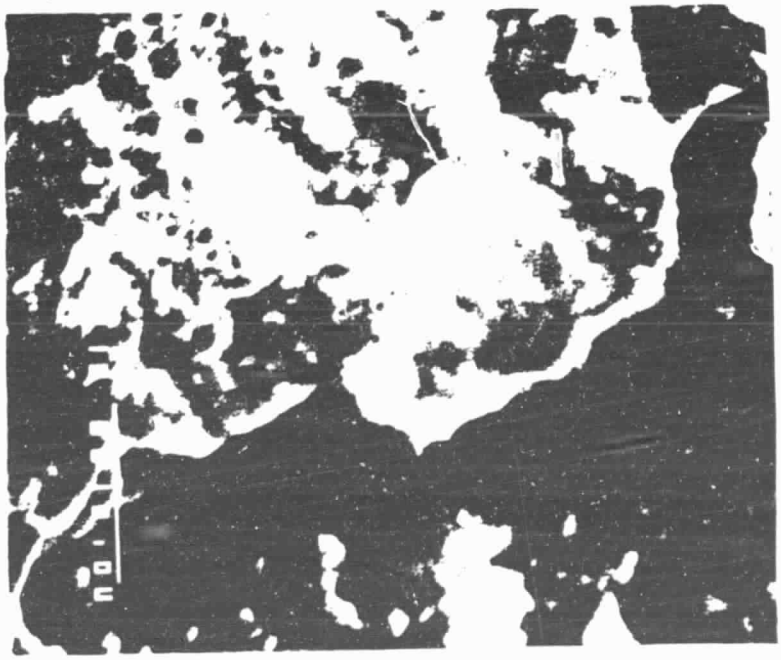

b) 2400X

Figure 55: Fracture surface of joint welded at 350 C, 2500 psi.

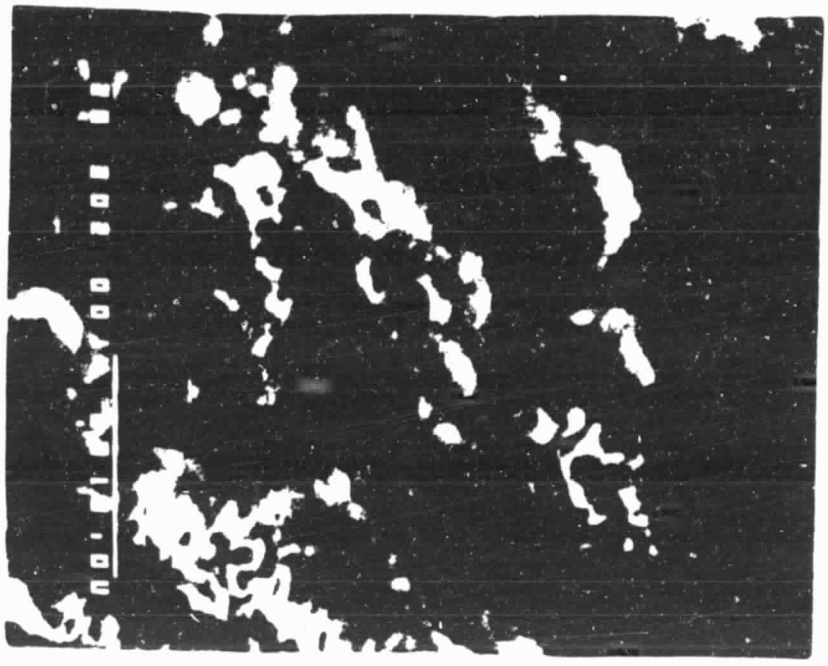

a) 3000X

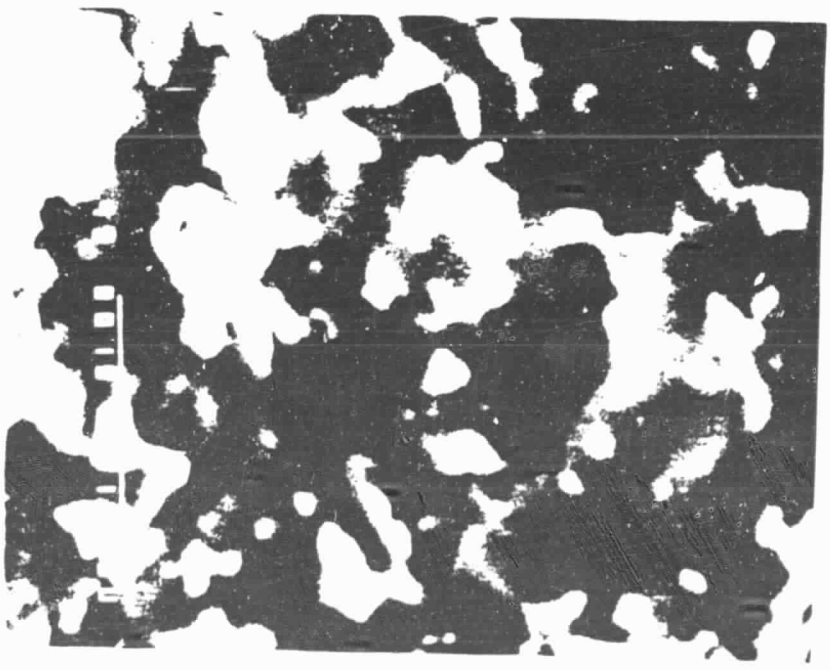

b) 3900X

Figure 56: Fracture surface of joint welded at 350 C, 2500 psi.

failure occurred at the interface between the coating and substrate, rather than within the substrate.

The influence of pressure is Illustrated by the SEM macrographs in figures 49 through 52. Contrary to the observations of Dini et.al.[67], changes in pressure appeared to have greater effect at higher temperatures. A doubling of the pressure at 250 C resulted in only a slight improvement in bonding. In comparison, doubling the pressure at 450 C altered the joint integrity from bonding in the outer ring only to a strength approaching the adherence of the silver coatings.

The effect of temperature on joint quality is also indicated by figures 49 through 52. Again, the effect of changing temperature was greater at higher pressures than at lower pressures. Adding these observations to the relationships developed in the first part of this study, the complete relationships between pressure, temperature and joint strength might be assumed to be as shown in figure 57.

Cracking. Perhaps the greatest difficulty encountered was the problem of cracking in the GaAs component. Since the scope of the study allowed only the temperature, pressure and time to be varied, the problem was not completely solved. However, the probable causes

of cracking were identified, and related to the welding parameters.

The applied welding pressure was of course one of the principal causes of cracking. It was demonstrated that damage could be eliminated by a sufficient reduction in pressure. The effect of pressure is intimately related to the surface condition, however, as the mechanism is assumed to be similar to fracture of a bent beam. This is illustrated in figure 58. Little data exists on the mechanical properties of GaAs, since it is not a structural material. It was therefore not possible to analytically determine the pressures and surface conditions which would result in cracking.

To illustrate the importance of surface preparation, the bending stress was calculated for several different surface conditions, using a pressure of 5000 psi and the following equation:[68]

$$\sigma_{max} = .280\ p\ a^2 / t^2$$

where $\sigma_{max}$ = maximum stress

p = pressure

a = support spacing

and t = thickness of part

The results are shown in table 6. The spacing between supports represents the surface condition, with the

Table 6: Stress on components as affected by surface condition.

| Support Spacing | Bending Stress From 5000 psi |
|---|---|
| .001" | 10 |
| .005" | 249 |
| .025" | 6625 |
| .050" | 24900 |

smaller numbers indicating a rough surface and larger numbers indicationg a wavy surface. From these calculations, the surface finish (roughness) has little effect on cracking, but a lack of flatness can be very significant.

Further evidence of the influence of surface condition on cracking was provided by the assemblies containing a Kovar pad. The surface preparation technique was much less stringent for the Kovar components than for the BeO components. In every case, cracking wwas much more significant in the Kovar assemblies than in those using BeO as the pad.

The welding temperature also had a considerable effect on cracking of the GaAs, because of the thermal expansion differential between the members of the stack. Cracking was observed to be more extensive and occur at lower pressures at higher welding temperatures.

The obvious response to the effect of temperature on cracking would be to deccrease the cooling rate to room temperature. This would be expected to reduce the thermal stresses through creep. Apparently, the creep rate was not sufficient at the temperatures used to cause stress relief within a reasonable period of time. The cooling time from 350 C was varied from 0.5 hour to

2 hours with no appreciable change in the cracking.

## CONCLUSIONS

As a result of the experimental work conducted in the first phase of the study, diffusion welding silver electroplated steel coupons, the following conclusions may be drawn:

1. Below 250 C welding temperature, reliable joint strength cannot be obtained, up to 25,000 psi welding pressure.

2. Up to about 300 C, increasing welding temperature significantly increases joint strength. Further increases in temperature result in only minimal strength improvement, for welding pressures above 10,000 psi.

3. Below 10,000 psi, strength drops markedly with decreases in pressure. Increasing pressure above 10,000 psi does not significantly affect the joint strength.

The second phase of the experimentation, using mockups of the Cassegrainian concentrator cell stack assembly, led to the following results:

1. Welds performed at higher pressures essentially supported the results from the first phase of the investigation. At lower pressure (2500 psi) temperature was significant over a wider range than at higher pressures. Weld quality improved significantly when the welding temperature was raised from 350 to 450 C.

2. Cracking in the GaAs layer was related to both temperature and pressure. The effect of pressure was, in turn, related to the surface quality. At 350 C welding temperature, the maximum pressure with no cracking was 1250 psi. Temperature was related to cracking because of the thermal expansion differential in the stack. Increasing the cooling time to 2 hours from 350 C did not noticably effect the cracking problem.

## RECOMMENDATIONS

The experimentation conducted in the present study indicates that diffusion welding holds some promise as a joining procedure for the Cassegrainian Concentrator Cell Stack Assembly. However, considerable work remains to be done in developing the procedure, especially in eliminating cracking. Surface preparation should be a primary consideration in future tests, as improvement in this area would both increase weld strength and decrease the tendency toward cracking.

In light of the problems encountered with the hot isostatic press, future developmental work might consider an alternate device such as the hybrid sketched in figure 48. The device could use a hydraulically actuated piston sliding through a cylindrical die, similar to the uniaxial systems described in the Review chapter. The cylinder, however, would contain the assemblies and a granular pressure transfer medium, so that the stress on the assemblies would resemble that produced by a HIP. Heating details are not shown, but one disadvantage of the system might be greater thermal gradients than those encountered with the HIP. The advantages of the hybrid system would be its simplicity, low cost, and possibly greater consistency.

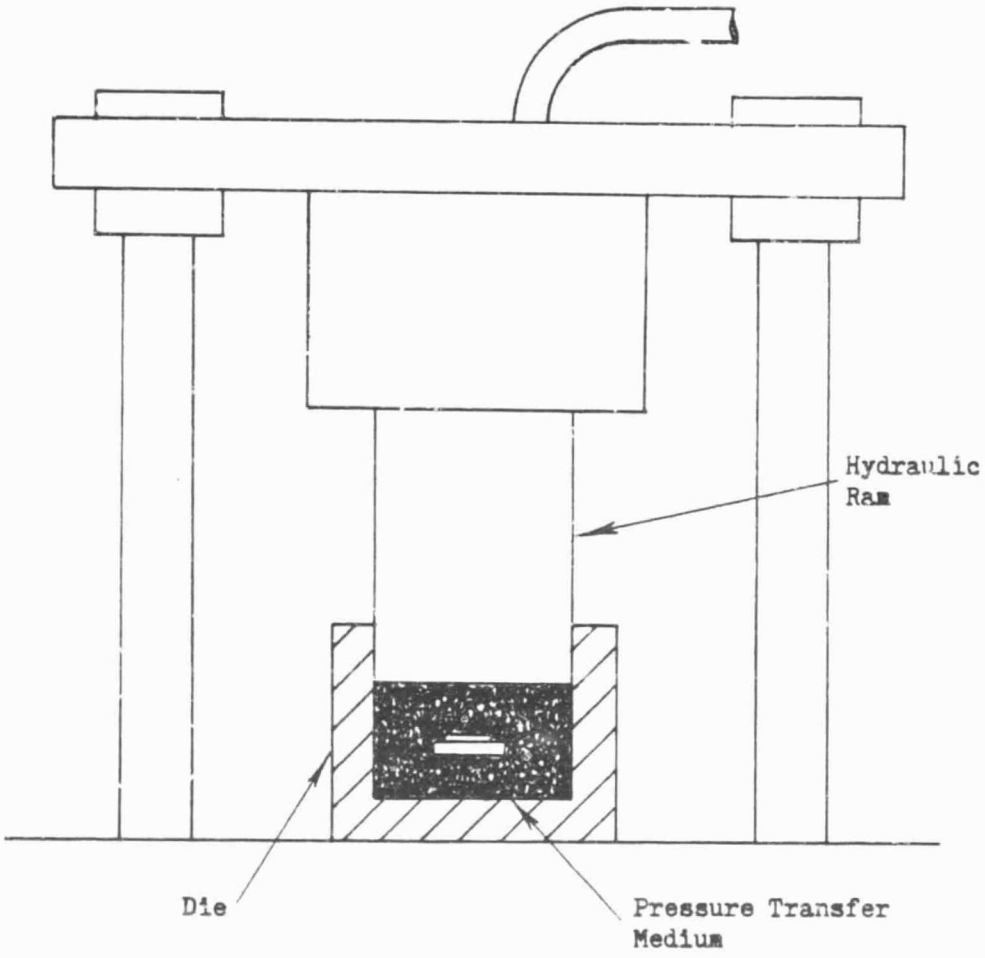


Figure 59: Diagram of hybrid pressure system for possible use in future experimentation.

A parallel effort in soldering the assemblies should also be considered, both for comparison with satisfactory diffusion welded assemblies and as a backup process should diffusion welding prove to be less than desirable.

## REFERENCES


1. R.E. Patterson and W.L. Crabtree. "Cassegrainian Concentrator Solar Array Exploratory Development Module." 17th IEEE Conference, August, 1982.

2. Meier, Daniel L. and Schroder, Dieter K. "Contact Resistance: Its Measurement and Relative Importance to Power Loss in a Solar Cell." IEEE Transactions on Electron Devices, V ED-31, N 5, May, 1984, p.647-653.

3. D.K. Schroder and D.L. Meier. "Solar Cell Contact Resistance-A Review." IEEE Transactions on Electron Devices." V ED-31, N 5, May,1984, p.637-646.

4. A. Ileadis and K.E. Singer. "The Role of Germanium in Evaporated Au-Ge Ohmic Contacts to GaAs." Solid State Electronics, V 26, N 1, 1983, p.7-14.

5. A. Christou. "Solid Phase Formation in Au:Ge/Ni, Ag/In/Ge,In/Au:Ge GaAs Ohmic Contact Systems." Solid State Electronics, V 22, 1979, p.141-149.

6. Y.S. Touloukian, R.K. Kirby, R.E. Taylor and P.D. Desai. Thermophysical Properties of Matter, V12, New York, NY, IFI Plenum, 1975.

7. Pampuch, Roman. Ceramic Materials: an Introduction to Their Propertied, New York, NY, Elsevier Scientific Pub., 1976.

8. A. Kaplan. "Fatigue Analysis of Solar Cell Welds." 10th PVSC, 1973.

9. The Welding Handbook, Volume 3,American Welding Society, Miami, Florida, 1980.

10. V.V. Abramov. "Kinetics of Plastic Deformation of Micro-Asperities of Copper and Nickel During Solid Phase Welding." Welding Prod.,1973, N 2, p. 4-7.

11. J.M Parks. "Recrystallization Welding." Welding Journal, May, 1953, p. 209-s to 221-s.

12. E.S. Karakozov. "Calculation of the Contact Surface in the Solid Phase Welding of Metals." Welding Prod. 1973, N 2, p. 83-86.

13. Reed-Hill,Robert E. Physical Metallurgy Principles. D. Van Nostrand Co., New York, NY, 1973.

14. Ibid.
15. Parks.

16. Abramov.

17. B. Derby and E.R. Wallach. "A Computer Model for Diffusion Bonding." Acta Metallurgica,

18. Dieter*

19. Karakozov.

20. D.G. Crawford. "The Joining of Aluminum and its Alloys to Similar and Dissimilar Materials by Diffusion Bonding- A Review." The Welding Institute, Cambridge, England, 1983.

21. Dieter.

22. Ibid.

23. Reed-Hill.

24. Parks.

25. Ibid.

26. Ibid.

27. Reed-Hill.

28. Ibid.

29. Ibid.

30. Ibid.

31. C.H. Crane, D.T. Lovell, W.A. Baginski and M.G. Olsen. "Diffusion Welding of Dissimilar Metals." Welding Journal, Jan., 1967, p. 23-s to 31-s.

32. Allison Butts and G.R. VanDuzee. "Low Temperature Bonding of Silver." Silver

33. Ibid.

34. J.W. Dini, W.K. Kelley, W.C. Cowden and E.M. Lopez. "Use of Electrodeposited Silver as an Aid in Diffusion Welding." Welding Journal, V 63, N 1, Jan., 1984, p.26-s to 34-s.

35. Butts

36. R.A Morley and J. Caruso. "The Diffusion Welding of 390 Aluminum Alloy Hydraulic Valve Bodies." Welding Journal, V 59, N 8, Aug., 1980, p. 29-34.

37. Dini.

38. E.R. Naimon, J.H. Doyle, C.R. Rice, D. Vigil and D.R. Walmsley. "Diffusion Welding of Aluminum to Stainless Steel." Welding Journal, V 60, N11.

39. Dini.

40. Crane.

41. Crawford.

42. M. O'Brien, C.R. Rice and D.L. Olsen. "High Strength Diffusion Welding of Silver Coated Base Metals." Welding Journal, Jan., 1976, p. 25-27.

43. Naimon.

45. Butts.

46. J.L. Knowles and T.H. Hazlett. "High Strength Low Temperature Bonding of Beryllium and Other Metals." Welding Journal, July, 1970, p.301-s to 310-s.

47. Ibid.

48. O'Brien.

49. Crane.

50. Knowles.

51. Crane.

52. Knowles.

53. Crane.

54. Knowles.

55. Naimon.

56. Crane.

57. Dini.

58. Morley.

59. O'Brien.

60. Knowles.

61. Butts.

62. Dini.

63. Knowles.

64. H.D. Hanes. "Plenary Lecture on Hot Isostatic Processing." Battelle Columbus Laboratories, Columbus, Ohio.

65. F.P.Beer and E.R. Russell. Mechanics of Materials, McGraw-Hill Book Co., New York, NY, 1981.

66. O.W. Blodgett. Design of Welded Structures, The James F. Lincoln Arc Welding Foundation, Cleveland, Ohio, 1982.

67. Ibid.

## APPENDIX

Raw Data From Gleeble Study

| Temp. ( C) | Load (lb.) | Diam. (in.) | Fail Strength (lb.) |
|---|---|---|---|
| 200 | 890 | .270 | 0 |
| 200 | 790 | .270 | 0 |
| 200 | 700 | .270 | 0 |
| 200 | 470 | .270 | 0 |
| 200 | 880 | .270 | 194 |
| 200 | 1120 | .270 | 0 |
| 200 | 1170 | .270 | 0 |
| 225 | 950 | .272 | 278 |
| 225 | 840 | .274 | 0 |
| 225 | 780 | .277 | 0 |
| 225 | 980 | .278 | 310 |
| 225 | 680 | .279 | 112 |
| 225 | 560 | .280 | 0 |
| 225 | 320 | .280 | 0 |
| 225 | 240 | .280 | 0 |
| 225 | 440 | .280 | 0 |
| 250 | 960 | .264 | 444 |
| 250 | 740 | .264 | 100 |
| 250 | 660 | .264 | 400 |
| 250 | 470 | .266 | 128 |
| 250 | 390 | .268 | 360 |
| 250 | 290 | .268 | 242 |
| 275 | 870 | .280 | 342 |
| 275 | 770 | .280 | 0 |
| 275 | 660 | .280 | 76 |
| 275 | 410 | .280 | 302 |
| 275 | 350 | .280 | 333 |
| 275 | 270 | .280 | 352 |
| 300 | 840 | .250 | 470 |
| 300 | 800 | .250 | 510 |
| 300 | 770 | .251 | 440 |
| 300 | 660 | .251 | 490 |
| 300 | 570 | .251 | 545 |
| 300 | 440 | .251 | 545 |
| 300 | 1270 | .258 | 630 |

| | | | |
|---|---|---|---|
| 300 | 1060 | .258 | 440 |
| 350 | 910 | .254 | 630 |
| 350 | 860 | .254 | 570 |
| 350 | 770 | .255 | 575 |
| 350 | 580 | .255 | 485 |
| 350 | 1040 | .256 | 575 |
| 350 | 1190 | .257 | 640 |
| 400 | 800 | .250 | 495 |
| 400 | 730 | .250 | 595 |
| 400 | 1020 | .250 | 580 |
| 400 | 700 | .250 | 485 |
| 400 | 980 | .250 | 510 |
| 400 | 830 | .250 | 510 |
| 400 | 690 | .250 | 585 |
| 400 | 600 | .250 | 360 |
| 400 | 940 | .250 | 580 |
| 400 | 730 | .250 | 505 |
| 400 | 860 | .250 | 470 |
| 400 | 700 | .250 | 595 |
| 400 | 480 | .250 | 660 |
| 400 | 600 | .250 | 545 |
| 450 | 1070 | .258 | 520 |
| 450 | 950 | .260 | 575 |
| 450 | 840 | .260 | --- |
| 450 | 860 | .261 | 515 |
| 450 | 770 | .262 | 490 |
| 450 | 680 | .262 | 520 |
| 450 | 610 | .264 | 480 |
| 500 | 940 | .252 | 590 |
| 500 | 870 | .252 | 610 |
| 500 | 740 | .252 | 510 |
| 500 | 680 | .253 | 500 |
| 500 | 490 | .253 | 510 |
| 500 | 380 | .253 | 450 |
| 500 | 270 | .280 | 350 |